For Reference

NOT TO BE TAKEN FROM THIS ROOM

For Reference

NOT TO BE TAKEN FROM THIS ROOM

Ex libris
universitatis
albertaensis

The University of Alberta
Printing Department
Edmonton, Alberta

THE UNIVERSITY OF ALBERTA

DETERMINATION OF LIQUID DIFFUSION COEFFICIENTS USING MULTIPLE INTERNAL REFLECTANCE INFRARED SPECTROSCOPY

A THESIS

SUBMITTED TO THE FACULTY OF GRADUATE STUDIES

IN PARTIAL FULFILMENT OF THE REQUIREMENTS OF THE DEGREE

OF MASTER OF SCIENCE

DEPARTMENT OF CHEMISTRY

BY

Ⓒ A. H. M. VANDER VOET

EDMONTON, ALBERTA

JULY, 1967

UNIVERSITY OF ALBERTA

FACULTY OF GRADUATE STUDIES

The undersigned hereby certify that they have read, and recommend to the Faculty of Graduate Studies for acceptance, a thesis entitled

DETERMINATION OF LIQUID DIFFUSION COEFFICIENTS
USING MULTIPLE INTERNAL REFLECTANCE INFRARED
SPECTROSCOPY

submitted by A. H. M. Vander Voet, B. Sc. in partial fulfilment of the requirements for the degree of Master of Science in Chemistry.

ABSTRACT

Liquid diffusion coefficients for systems approximating gas chromatographic sample -- liquid phase systems were determined by using multiple internal reflectance infrared spectroscopy. An expression for the diffusion coefficient as a function of the change of concentration with time was developed from Fick's second law and Jost's treatment for diffusion into a slab. By using cell covers designed for this project (for FMIR solid sampling cell) and by turning the spectrophotometer (Infracord) on its side, it was possible to measure the change of concentration of solute (fed as vapour in carrier gas) in a layer of solvent with time spectrophotometrically and to thus determine the diffusion coefficient of the solute-solvent system. The systems used in the project included those of different solutes in fluorolube and acetone in solvents of varying viscosities.

An attempt was made to qualitatively evaluate the data by correlation with known values and values expected from empirical expressions. The results indicate that this method provides qualitative values for diffusion coefficients with main errors due to the preparation of the solvent layer.

ACKNOWLEDGEMENTS

The author wishes to thank Dr. W. F. Allen for his guidance and encouragement during the course of this project.

Thanks are also extended to the other staff members and students who assisted in this project. Special thanks are extended to R. Swindlehurst and the spectroscopy laboratory for their assistance with this project and to Jan Jordan for typing the final draft.

Financial assistance from the University of Alberta is gratefully acknowledged.

TABLE OF CONTENTS

Abstract iii

Acknowledgements iv

List of Tables vi

List of Figures ix

List of Symbols xi

I. INTRODUCTION

I-1 Liquid Phase Mass Transfer Term in Gas Chromatography 1

I-2 Diffusion 7

I-3 Reflectance Spectroscopy 17

II. EXPERIMENTAL

II-1 Reagents 30

II-2 Design of Apparatus 31

II-3 Verification of Beer's Law for FMIR 39

II-4 Measurements of Diffusion Coefficients 41

II-5 Comparison of the Rate of Sample Delivery to the Surface with Rate of Diffusion into the Liquid 47

III. RESULTS AND DISCUSSION

III-1 Experimental Results 54

III-2 Discussion 72

III-3 Errors 79

IV. CONCLUSION 84

BIBLIOGRAPHY 85

LIST OF TABLES

I. Values of C_1 and d_f^2/D_1 found by Eluting Propane, Isobutane and n-Butane on a Column of n-Octadecane on Sil-O-Cel C22 Using H_2 and N_2 as Carrier Gases 5

II. Values of C_1 Found by Eluting Acetone and Benzene on Columns With Varying Support Size of Polyethylene Glycol on Sil-O-Cel Using H_2 and N_2 as Carrier Gases 6

III. Wilke-Chang Association Parameters for Selected Solvents 15

IV. Atomic Volumes for Complex Molecules 16

V. Properties of Prism Materials for Reflectance Spectroscopy 25

VI. Critical and Safe Indices for KRS-5, AgCl, and Germanium 28

VII. Absorption at 3.4 Microns of Solutions of Dodecane in Fluorolube at Various Concentrations . 42

VIII. Absorption at 3.4 Microns of 0.26 M Solution of Dodecane in Fluorolube at Various Coverages of the Plate 44

IX. Absorption at 5.75 Microns of solutions of Acetone in Carbowax 600 at Various Concentrations . 52

X. Slopes (dA/dt/ and Logarithms of Slopes of the Tangents to the Absorbance Versus Time Plots .. 61

XI. Diffusion Coefficients for Systems Illustrated by Spectra and Calculated from the Slopes of the Log dA/dt Versus Time Plots 63

XII. Values of Log(dc/dt/ t and Diffusion Coefficients for 1-Pentene in Fluorolube Found Experimentally Using CC-B and Spacer Thicknesses 127 and 254 Microns 64

XIII. Values of Log(dc/dt)/ t and Diffusion Coefficients for 1-Pentene in Fluorolube Found Experimentally Using CC-B and Spacer Thicknesses 381 and 584 Microns 65

XIV. Values of Log(dc/dt)/ t and Diffusion Coefficients for 2-Methylbutane in Fluorolube Found Experimentally Using CC-B and Spacer Thicknesses 127 and 254 Microns 66

XV. Values of Log(dc/dt)/ t and Diffusion Coefficients for 2-Methylbutane in Fluorolube Found Experimentally Using CC-B and Spacer Thicknesses 381 and 584 Microns 67

XVI. Values of Log(dc/dt)/ t and Diffusion Coefficients for Diethyl Ether in Fluorolube Found Experimentally Using CC-B and Spacer Thicknesses 127 and 254 Microns 68

XVII. Values of Log(dc/dt)/ t and Diffusion Coefficients for Diethyl Ether in Fluorolube Found Experimentally Using CC-B and Spacer Thicknesses 381 and 584 Microns 69

XVIII. Summary of Values of Diffusion Coefficients for 1-Pentene, 2-Methylbutane and Diethyl Ether in Fluorolube 70

XIX. Values of Diffusion Coefficients for Acetone in Carbowax 600, Carbowax 1500, Silicone Grease, Dinonylphthalate, and Ucon 71

XX. Errors in Absorbance Due to Transformation of Data From Percent Transmittance to Absorbance Units 81

XXI. Errors Found in Replotting Data 83

LIST OF FIGURES

1. Plot of integral equation (x) for diffusion into a plate 12
2. Penetration depth into the rarer medium versus the angle of incidence at wavelength 3.4 microns 20
3. Apparent path of radiation in total internal reflection 20
4. Anomolous Dispersion 22
5. Internal reflection bands resulting from levels of plate refractive indices relative to the refractive index of the sample 22
6. Schematic diagram of FMIR optical system 24
7. Schematic diagram of spectrophotometer as supported on its side. 32
8. Schematic diagram of cell cover CC-A 34
9. Schematic diagram of cell cover CC-B 35
10. Spacer, top view, and baffle system for CC-B cavity . 36
11. Sampling system 38
12. Spectrum analysis for calculation of Beer's law plot .40
13. Beer's law plot, Absorbance versus concentration, for solutions of dodecane in fluorolube 43
14. Beer's law plot of absorption versus path length or coverage of the plate 44
15. Vapour pressure curves for 1-pentene and acetone 49

16. Beer's law plot, absorbance versus concentration for solutions of acetone in Carbowax 600 52

17. Spectrum of diethyl ether in fluorolube at wavelength 3.4 microns (CC-B, 254 micron spacer) 55

18. Spectrum of 2-methylbutane in fluorolube at wavelength 3.4 microns (CC-B. 584 micron spacer).........56

19. Spectrum of 2-methylbutane in fluorolube at wavelength 3.4 microns (CC-B, 381 micron spacer) 57

20. Replot of figure 17 as absorbance versus time with slopes of tangents at various times constructed 58

21. Replot of figure 18 as absorbance versus time with slopes of tangents at various times constructed 59

22. Replot of figure 19 as absorbance versus time with slopes of tangents at various times constructed 60

23. Plots of log dc/dt versus time for the absorbance versus time plots shown in figures 20. 21 and 22 62

24. Wilke-Chang dependence of D on $1/V^{0.6}$ 76

SYMBOLS

A	Eddy diffusion term in the Van Deemter equation
A	Absorbance in Beer's law expression
B	Gas diffusion term in the Van Deemter equation
C_g	Gas phase mass transfer term
C_l	Liquid phase mass transfer term
D_g	Gas diffusion coefficient, cm^2/sec
D_l, D	Liquid diffusion coefficient, cm^2/sec
F_g	Volume fraction in gas phase
F_l	Volume fraction in liquid phase
H	Height equivalent to a theoretical plate
J	Flux of solute across unit area fixed in solvent
K	Distribution coefficient
N	Avogadro's number
R	Gas constant
T	Percent transmission
T	Absolute temperature

V	Molal volume of solute at normal boiling point in Wilke-Chang equation, cc/gm mole
a	Absorptivity
b	Path length
c	Concentration
c	Partition coefficient in Golay equation
d_f	Thickness of liquid phase on support, cm
d_p	Average particle diameter, cm
h	Thickness of slab, cm
k'	Function of distribution coefficient such that $k = K(F_l/F_g)$
r_o	Radius of capillary in Golay equation
r_1	Radius of diffusing molecule in Stokes-Einstein equation
n_r	Refractive index of rarer medium
n_d	Refractive index of denser medium
t	Time, sec
u_o	Velocity of carrier gas

x	Association parameter in Wilke-Chang equation
x	Distance
λ	Factor relating to irregularities in packing
γ	Correction for tortuosity
θ_c	Critical angle

1 INTRODUCTION

The research described in this paper arose from interest in two areas of instrumental analysis, namely gas chromatography and FMIR (Frustrated Multiple Internal Reflectance) infrared spectroscopy. Interest in the liquid mass transfer term in gas chromatography and subsequent reading led to the conclusion that there is very little data available concerning diffusion coefficients in chemical systems applicable to chromatography. Research has been done in this field but due to the lack of numbers, only qualitative results have been obtained. It seemed possible to use the technique of reflectance spectroscopy to measure diffusion coefficients of systems similar to the sample -- liquid support systems of gas chromatography and perhaps provide some numbers for the mass transfer term.

1-1. Liquid Phase Mass Transfer Term in Gas Chromatography

In gas chromatography column efficiency is most often expressed in terms of HETP (Height Equivalent to a Theoretical Plate). The value of H for a particular system is usually considered to be dependent on three factors: diffusion spreading (longitudinal spreading of the plug of solute molecules in the mobile phase), eddy diffusion (caused by variations in flow velocity at

different points in the packing caused by the packing) and the resistance to mass transfer in both the mobile and stationary phase. Van Deemter, Zuiderweg, and Klinkenberg (22) expressed this dependency mathematically; in its simpler form this relationship is

$$H = 2\lambda d_p + \frac{2\gamma D_g}{u_o} + \frac{2k' d_f^2 u_o}{3(1+k)^2 D_l}$$

or as more commonly written $H = A + B/u_o + C_l u_o$, (15)

where -

u_o - the average velocity of the carrier gas

A - the eddy diffusion term

d_p - the particle diamenter

λ - a factor relating to the irregularities in column packing

B - gas diffusion term

D_g - gas diffusion coefficient

γ - tortuosity correction

C_l - liquid phase mass transfer term

D_l - liquid diffusion coefficient

k' - distribution coefficient function

d_f - average thickness of the liquid phase on the solid support.

The value of k' is defined by the distribution coefficient K, the volume fraction occupied by the gas phase F_g, and the volume fraction occupied by liquid phase F_l so that $k' = K (F_l/F_g)$ (20).

The mass transfer term C_l as given above was derived (21) without any special regard to the type of column or application of solvent in the column. One special case, which may occur in packed columns and which is generally assumed in capillary columns is that of a continuous film. The C_l term defined by Golay for columns (13) is

$$\frac{k^3 u_o r_o^2}{6 (1+k)^2 F^2 c^2 D_l}$$

where r_o is the radius of the capillary, k is the distribution coefficient term, F is a constant of proportionality used in the determination of effective area, and c is the partition coefficient.

In both expressions for C_l it is seen that the mass transfer term is directly proportional to the square of the thickness of the layer of liquid phase and to the velocity of the carrier gas; and it is inversely proportional to the diffusion coefficient in the liquid phase.

Work has been done in separating the C_l term from the general rate equation and finding experimental values for it.

Barr and Sawyer (1) found the functional dependence of C_1 on k (or k'), and found the effect of different carrier gases on the value of the k term. Perrett (19) in studying the effect of column repacking on the values of C_1 and C_g (where C_g is the term corresponding to the resistance to mass transfer in the gas phase used in the extended Van Deemter equation) found values of k and C_1, and from these calculated values of d_f^2/D_1 (Table 1). To calculate the values of d_f^2/D_1 he assumed the Van Deemter term dependence of C_1 on k as $f(k) = 2k/3(1\ k)^2$. He states that this f(k) seemed to give reasonable values of d_f^2/D_1 but that the lack of independent diffusion coefficient data provided only qualitative results. Bohemen and Purnell (3) calculated values of C_1 using various particle sizes of solid support (Table 11) and finding a constant value of d_f^2/D_1 for all runs concluded that for fine particles d_f was independent of particle size. In arriving at these conclusions these authors assumed the value of the diffusion coefficient of acetone in polyethylene glycol to be 10^{-7} cm^{2}sec^{-1}. Evanoff (7) studied the effect of solvent and temperature on diffusion coefficients of some organic nitro-compounds using polarography and viscosity measurements.

The work quoted above is representative of what has been done and indicates the lack of independent diffusion coefficient data for these systems. For this reason this

TABLE 1. VALUES OF C_1 AND d_f^2/D_1 FOUND BY ELUTING PROPANE, ISOBUTANE AND n-BUTANE ON A COLUMN OF n-OCTADECANE ON SIL-O-CEL C22 MESH RANGE 100-120 BSS USING H_2 AND N_2 AS CARRIER GASES (19)

Column	Carrier gas	$C_1 \times 10^4$, sec			$d_f^2/D_1 \times 10^3$, sec		
		C_3	i-C_4	n-C_4	C_3	i-C_4	n-C_4
1 A	H_2	13±1	16±1	11±1	8.1±1	13.5±1	11.8±1
	N_2	16	15	12	10	12.6	12.9
I B	H_2	16	14	11	10	11.8	11.8
	N_2	16	15.5	11	10	13.0	11.8
I C	H_2	15	16	11	9.4	13.4	11.8
	N_2	13	16	12	8.1	13.4	12.9

TABLE 11. VALUES OF C_1 FOUND BY ELUTING ACETONE AND BENZENE ON COLUMNS WITH VARYING SUPPORT SIZE OF POLYETHYLENE GLYCOL[a] ON SIL-O-CEL USING H_2 AND N_2 AS CARRIER GASES (3)

Sil-O-Cel Support Size, d_p, cm	Carrier gas	$C_1 \times 10^3$, sec Acetone	Benzene
0.032	H_2	2.4	2.9
	N_2	2.4	2.9
0.016	H_2	1.1	1.6
	N_2	1.1	1.6
0.010	H_2	1.2	1.5
	N_2	1.2	1.5

[a] 20 percent w/w

work was begun to try to find a way of providing numbers which could give more information about phase thicknesses, about C_1 itself and its functional dependence on k.

1-2. Diffusion

Diffusion is a process which leads to the equalization of concentrations within a single phase. The laws of diffusion connect the rate of flow of the diffusing substances with the concentration gradient responsible for this flow. The principle rules which govern diffusion are Fick's laws (6). Fick's first law states that the flux J of a given component or solute across a unit area fixed in the medium is:

$$J = -D\, \partial c / \partial x$$

where D is the diffusion coefficient in units $cm^2 sec^{-1}$ and $\partial c / \partial x$ is the concentration gradient. Often it is not possible to investigate diffusion coefficients under conditions of a constant concentration gradient; instead, it is preferable to study the change of concentration with time within the medium. When there is diffusion in the x-direction only, and if the rate of increase in the amount of substance within a volume element bounded by two parallel planes of unit area situatex at x and $x+dx$ is observed, this increase is equal

to the amount diffusing into the volume element minus the amount diffusing out of it per unit time, that is $J_x - J_{x+dx}$. Thus the rate of accumulation in the volume element is:

$$J_x - J_{x+dx} = -D\,(\partial c/\partial x)_x - (-D\,(\partial c/\partial x)_{x+dx})$$
$$= -(\partial J/\partial x)\,dx.$$

The rate of concentration increase $\partial c/\partial t$ is the accumulation rate per unit volume $(J_x - J_{x+dx})/dx$, i.e.,

$$\partial c/\partial t = -\partial J/\partial x.$$

Substituting for J from Fick's first law the expression

$$\partial c/\partial t = D\,\partial^2 c/\partial x^2$$

is obtained, which is Fick's second law of diffusion (9). In Fick's second law the diffusion coefficient is assumed constant.

The experimental system in this work is approximated by a slab bounded by two planes perpendicular to the x-axis (either of infinite dimensions) or bounded by an impermeable surface of arbitrary shape but parallel to the x-axis. In this bounded system the initial and boundary conditions are only dependent on x.

For diffusion into a slab Jost (16) begins the solution of Fick's second law by putting concentration as a function of time and distance, i.e.,

$$c = X(x)\ T(t). \qquad \text{(i)}$$

This makes the second law

$$X\ T' = D\ T\ X'' \qquad \text{(ii)}$$

where the primes refer to the differentiation with respect to the corresponding variables. Thus it can be written in the form:

$$T'/T = DX''/X. \qquad \text{(iii)}$$

These can only be equal if they are equal to the same constant which is chosen to be $-\lambda^2 D$. Thus, $T'/T = -\lambda^2 D$ and $X''/X = -\lambda^2$ with solutions to the differential equations being

$$T \sim \exp(-\lambda^2 Dt) \qquad \text{(iv)}$$

$$X = A \cos \lambda x + B \sin \lambda x. \qquad \text{(v)}$$

If the solution is to be finite for all values of t, then λ^2 must be greater than zero.

For the unbounded (infinite) linear system, A and B are considered to be functions of λ, and expression (i) is integrated

$$c \quad \int_0^\infty A(\lambda) \cos \lambda x + B(\lambda) \sin \lambda x \exp(-\lambda^2 Dt)\ d\lambda\ . \qquad \text{(vi)}$$

For the bounded system the concentration is again considered to be a function of time and distance and solutions (iv) and (v) are again obtained. Where in the

infinite case λ was restricted only by the condition $\lambda^2 > 0$, in the bounded case it is restricted further and only allowed positive integral values. The integral for c is now represented by an infinite sum over all discrete values of λ instead of as before, by an integral over the continuously varying values of λ.

Specific examples for diffusion out of and into a slab are treated here because of their special applicability to this work.

For the diffusion out of a slab it is necessary to set up the proper boundary conditions which are:

$c = c_o$ for $0 < x < h$ at $t = 0$,

$c = 0$ for $x = 0$ and $x = h$ at $t > 0$

(i.e., diffusion from both sides of the slab).

From expression $c = (A \sin \lambda x + B \cos \lambda x) \exp(-\lambda^2 Dt)$ it is seen that the boundary conditions are fulfilled for $B = 0$ and $\lambda = n\pi/h$.

The general solution is now

$$c = \sum_{n=1}^{\infty} A_n \exp\left[- \frac{n^2\pi^2 Dt}{h^2} \right] \sin n\pi x/h. \qquad \text{(vii)}$$

The arbitrary constants A_n must be determined in such a way as to conform with the initial conditions, i.e.,

$$c_o = \sum_{1}^{\infty} A_n \sin n\pi\, x/h \qquad \text{for } 0 < x < h \text{ at } t=0. \quad \text{(viii)}$$

Jost uses Fourier's theorem and arrives at the solution

$$c = 4c_0/\pi \sum_{v=0}^{\infty} (1/2v+1) \sin \frac{(2v+1)\pi x}{h} \exp\left[-\left(\frac{(2v+1)\pi}{h}\right)^2 Dt\right] \quad \text{(ix)}$$

$v = 0, 1, 2, 3 \ldots$

When the solution is plotted as c versus x for different times, it is seen (17) that the curves are symmetrical around h/2, which is to say that there is no diffusion across the midpoint of the slab.

For the problem of diffusion into a slab the solutions are easily derived from the above by consideration of the new boundary conditions i.e., $c = c_0$ at $x = 0$ and at $x = h$, for t greater than zero. If (ix) is a solution of Fick's second law, the negative of it is also a solution. If c is a solution as in (ix), then $c_0 - c$ is the solution of the negative problem. Thus the solution for diffusion into a slab is given as

$$c = c_0 \left\{1 - 4/\pi \sum_{v=0}^{\infty} \frac{1}{2v+1} \sin \frac{(2v+1)\pi x}{h} \exp\left[-\left(\frac{(2v+1)\pi}{h}\right)^2 Dt\right]\right\} \quad \text{(x)}$$

If c were to be plotted versus x at various times, the plot would resemble that shown in fig. 1, and be symmetrical around the mid-point of the slab (i.e., at h/2)

The same effect could also be caused by an impermeable membrane at h/2. Thus, if diffusion through only

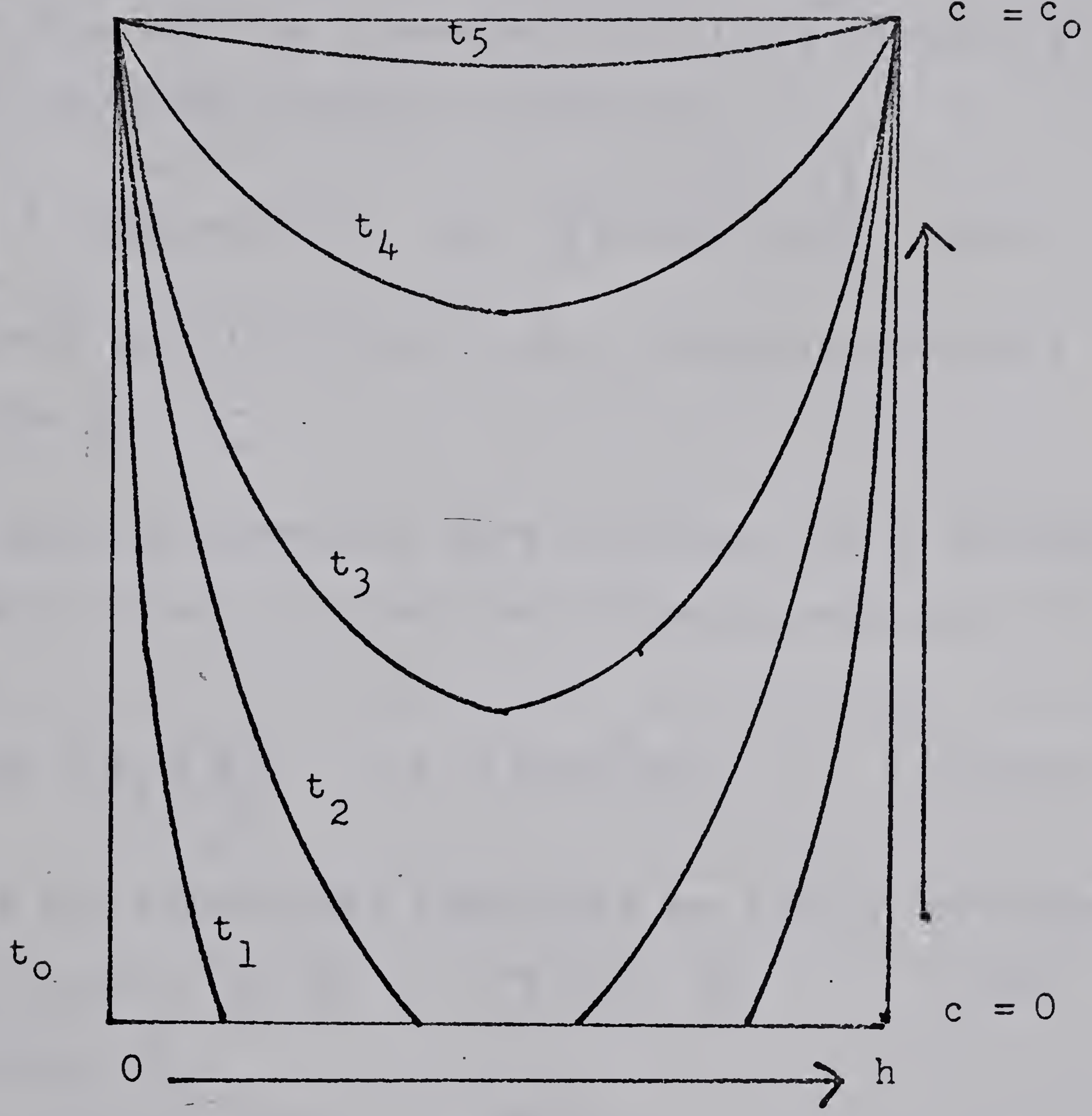

Figure 1. Plot of integral equation (x) for diffusion into a plate, the concentration at the boundaries being kept at c_o

one face of the slab is to be considered, the function need only be taken for $0 < x < h/2$. If expression (x) is approximated to the first order ($v = 0$) the resulting expression is:

$$c = c_o \left[1 - 4/\pi \ \sin \pi x/h \ \exp\left(- (\pi/h)^2 \ Dt\right)\right], \ 0 < x < h/2. \qquad \text{(xi)}$$

Since in this work the concentration will be measured at h/2, the expression reduces further to

$$c = c_o \left[1 - 4/\pi \ \sin \pi/2 \quad \exp \ -\left((\pi/h)^2 \ Dt\right)\right] \qquad \text{(xii)}$$

which should give the value of the concentration at h/2 at any time t.

To make the expression more tractable, it is differentiated with respect to t and the following expression is obtained:

$$dc/dt = c_o \frac{4\pi D}{h^2} \qquad e^{-(\pi/h)^2 Dt}. \qquad \text{(xiii)}$$

To remove the exponential logarithms are taken, obtaining

$$\ln (dc/dt) = \ln (K) + (-\pi^2/h^2) \ \ Dt \qquad \text{(xiv)}$$

which reduces to

$$\log (dc/dt) = (\log K) \ - \frac{\pi^2 Dt}{2.3 \ h^2} \qquad \text{(xv)}$$

in which log (dc/dt) is a linear function of t.

Thus if plots of concentration versus time are taken, their slopes at various values of t can be measured; and if the base ten logarithms of these slopes

are plotted against time, the result should be a straight line from whose slope the diffusion coefficient can be calculated.

Diffusion coefficients have been calculated from expressions relating diffusion to more measureable physical properties, especially viscosity. The first equation which had any success was the Stokes-Einstein equation (10):

$$D_1 = RT/6\pi r_1 \eta N$$

where r_1 is the "radius" of the solute molecule, N is Avogadro's number, η is the viscosity in centipoise, R the gas constant, and T the absolute temperature. This equation, however, was derived for particles of size greater than the solvent molecules, i.e., Brownian (colloid) particles. When the diffusing particles are almost the same size as the solvent molecules, a slippage factor is introduced and the 6 replaced by 4. Many other empirical expressions have been derived such as the Wilke-Chang equation (11) (23)

$$D_1 = 7.4 \times 10^{-8} \frac{(xM)^{\frac{1}{2}} T}{\eta V^{0.6}}$$

where x is an association parameter which is introduced to define the effective molecular weight of the solvent with respect to the diffusion process (see Table 111), M is the molecular weight of the solvent, T is the absolute

TABLE 111. WILKE-CHANG ASSOCIATION PARAMETERS FOR SELECTED SOLVENTS (23)

Solvent	Association Parameter
Water	2.6
Methyl Alcohol	1.9
Ethyl Alcohol	1.5
Benzene	1.0
Ether	1.0
Heptane	1.0

TABLE lV. ATOMIC VOLUMES[a] FOR COMPLEX MOLECULES (23)

Bromine	27.0
Carbon	14.8
Chlorine	24.6
Hydrogen	3.7
Iodine	37.0
Nitrogen, double bonded	15.6
Nitrogen, in primary amines	10.5
Nitrogen, in secondary amines	12.0
Oxygen (except as noted below)	7.4
Oxygen, in methyl esters	9.1
Oxygen, in methyl ethers	9.9
Oxygen, in higher esters and ethers	11.0
Oxygen, in acids	12.0
Sulphur	25.6
For three-membered ring, as in ethylene oxide, deduct	0.6
For four-membered ring, as in cyclobutane, deduct	8.5
For five-membered ring, as in furan, thiophene, deduct	11.5
For pyridene, deduct	15
For benzene ring,deduct	15
For naphthalene ring, deduct	30
For anthracene ring, deduct	47.5

[a] atomic contributions to the molal volume (at normal boiling point) for complex molecules.

temperature and V is the molal volume of the solute at normal boiling point measured in cc/gm mole. The value of V in the equation is estimated from Table lV.

In this work the calculation of diffusion coefficients relies on one basic assumption, that used by Golay (13): the rate of transport of solute molecules across the solvent surface is considered kinetically faster than the diffusion process and thus has no effect on the apparent value of the diffusion coefficient.

1-3 Reflectance Spectroscopy

As Fick's second law expresses the diffusion as a function of dc/dt, it remains to measure this quantity. Spectroscopy is useful in determining concentrations through the linearity of the Beer-Lambert law, which relates the absorbance of a species to its concentration by the relationship $A = abc$ (A-absorbance, a-absorptivity, b-path length, c-concentration). Normal transmission spectroscopy, by the nature of its sampling methods, would require that samples in a diffusion experiment be selected at known times and analyzed individually to give a point-by-point plot of concentration versus time. Problems such as the actual selection of samples, of transfer, and of spectroscopic sampling would seriously affect the credibility of the results. Ideally the diffusion experiment should

take place in the sampling area of the spectrophotometer to provide both immediate and continuous analysis. On the basis of the desired conditions for the experiment it was decided that reflectance spectroscopy, particularly Multiple Internal Reflectance, would be the most useful technique for analysis. The reasons for its usefulness will be discussed after a note on the theory of reflectance spectroscopy.

Internal reflection may be compared to external reflection as follows: in external reflection the incident beam travels through a medium of lower refractive index and is reflected from the surface of a medium of higher refractive index. In internal reflection the beam travelling through a medium of higher refractive index is reflected from the surface of a medium of lower refractive index. Furthermore, a critical angle is defined for any pair of media as the angle between the incident beam and the normal to the surface of the reflecting medium such that sine $\theta_c = n_r/n_d$ (θ_c - critical angle, n_r - refractive index of the rarer medium, n_d - refractive index of the denser medium). At angles less than θ_c, total internal reflection ceases; at angles θ_c to grazing, total internal reflection occurs.

With both internal and external reflection retention of most of the energy of the incident beam is expected after multiple reflections. However, Harrick (14) found for external reflections from a silvered surface, that after ten reflections there was a retention of only 3/5 of the total power; and that after the same number of reflections from a semi-conductor, he found a retention of 3.7×10^{-5} initial power. With internal reflections he found that for a silicon surface there was a retention of 50 per cent after more than 100 reflections.

A phenomenon of total internal reflection is the penetration of the incident beam and subsequently reflected beams (in multiple internal reflectance) into the rarer medium (that with lower refractive index) (14). Maxwell's theory predicts a penetration of the totally reflected power although there is no net flow or propagation into the rarer medium. The depth of penetration is directly proportional to the wavelength of the light in the denser medium and is inversely proportional to the ratio n_r/n_d (see fig.2). Because of the penetration of the totally reflected power across the surface, it is convenient to represent the path of the radiation as shown in Fig. 3. It must be remembered that this is not the actual path of the radiation since there is no propagation into the rarer medium.

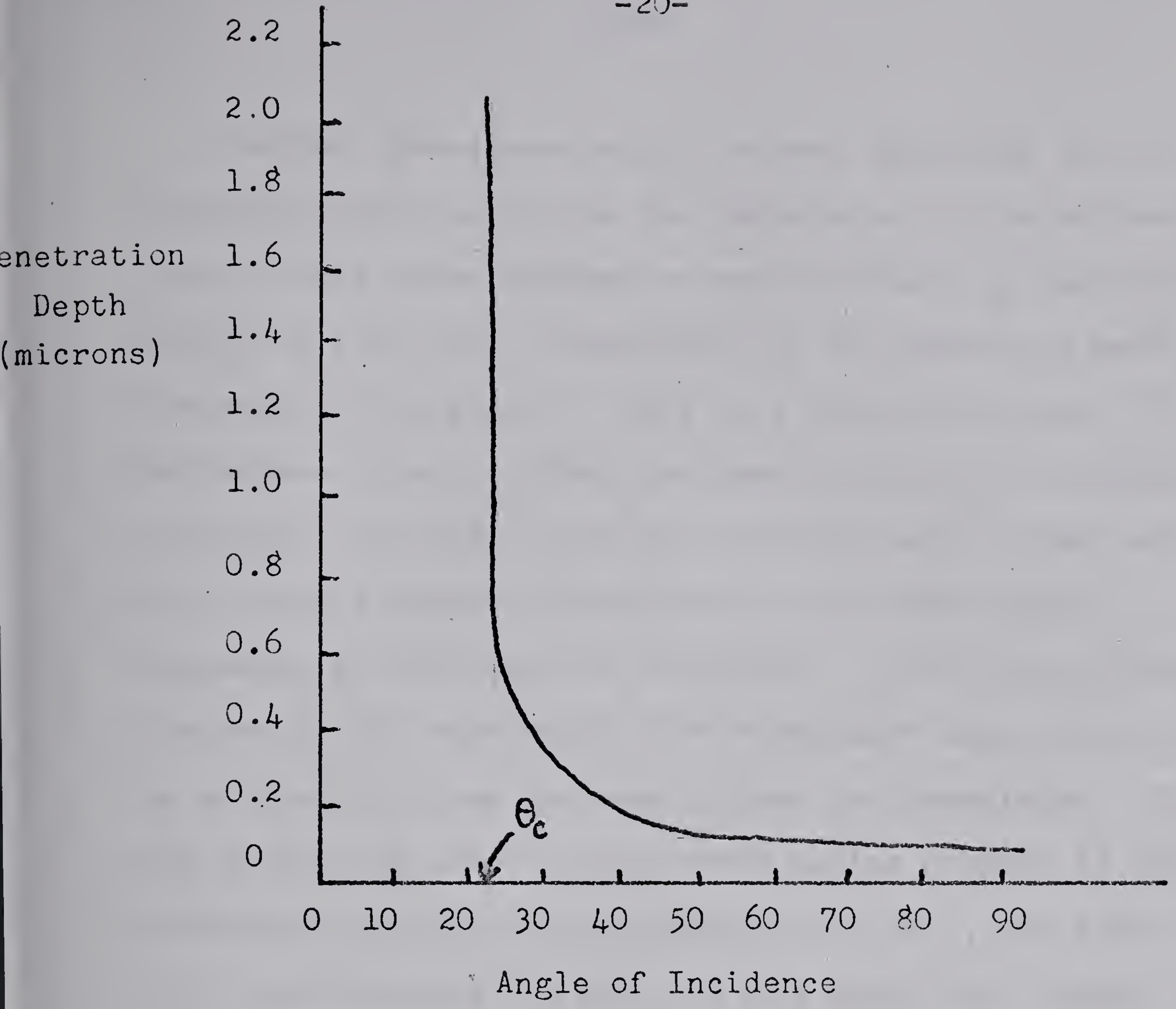

Figure 2. Penetration depth into the rarer medium versus the angle of incidence at a wavelength of 3.4 microns (14)

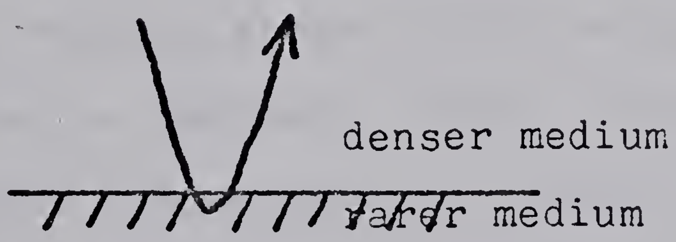

Figure 3. Apparent path of radiation in total internal reflectance

Another phenomenon which is very important in reflectance spectroscopy is the dependence of the refractive index of the rarer medium (or any material) on the wavelength of the light - especially at an absorption band in the medium (see fig.4). Thus in a dielectric plate of refractive index n_p, when the beam is totally internally relected at an angle near the critical angle, there will be a certain amount of penetration into the medium, depending on the angle of incidence. If the rarer medium absorbs at the wavelength of the incident beam, there will be an absorption of the energy that has penetrated. Since the refractive index of the rarer medium changes at the absorption band (anomalous dispersion) (2), the ratio n_r/n_d also changes and the critical angle will change. If the original angle of incidence is near or at the critical angle, the new critical angle will be less than the original, the angle of incidence will be greater than the new critical angle and total reflection will cease. If the wavelength is scanned past the absorption band, the refractive index returns almost to its original value and total reflection is resumed. If the intensity of reflected light is followed spectrophotometrically, a reflectance spectrum of the rarer medium is obtained. (25).

There are two basic forms of reflectance spectroscopy in the infrared region, namely Attenuated Total Reflectance

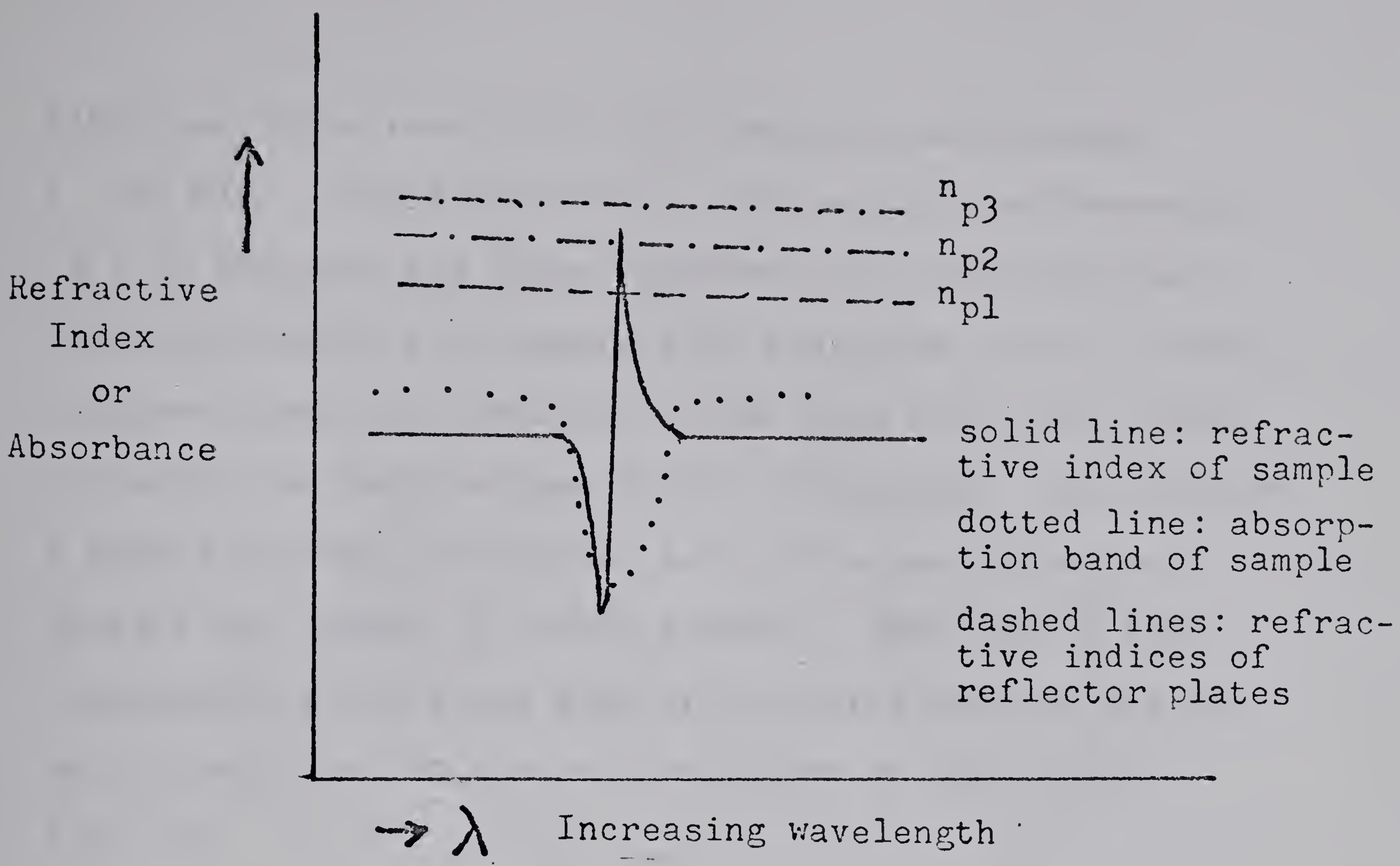

Figure 4. Anomolous dispersion - behaviour of refractive index of sample at an absorption band (25)

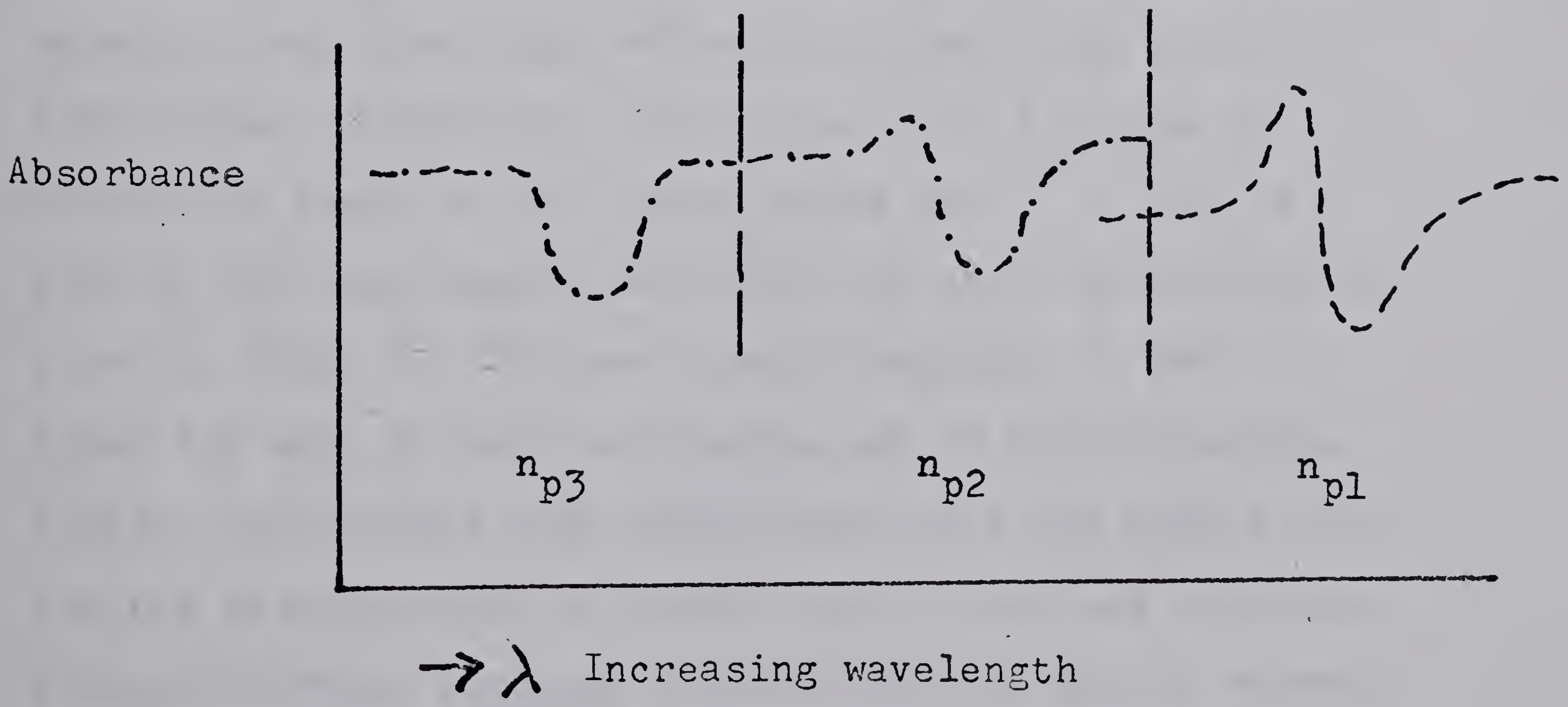

Figure 5. Internal reflection absorption bands resulting from the level (n_{p1}, n_{p2}, n_{p3}) of the plate refractive index relative to the refractive index of the sample (25)

(ATR) and (Frustrated) Multiple Internal Reflectance ((F) MIR). The first work in ATR was done by Fahrenfort (8) in 1961 and has since expanded until today ATR and FMIR attachments are commercially available to fit in most infrared spectrophotometers (single beam and double beam), including the Perkin-Elmer IR-137 (Infracord). ATR utilizes a single internal reflection in a prism against whose surface the sample is firmly pressed. FMIR uses a long rectangular prism plate with up to 25 reflections against which sample may be placed - on either or both sides. (fig. 6)

The choice of prism materials is one of the most important considerations in both ATR and FMIR, the prism material requiring high refractive index, high purity, high polish, durability, inertness, and of course no absorption bands in the region being used. A list of some of the most common materials and their properties is given in Table V. The most useful material in FMIR is KRS-5 (42 mole % Thallium bromide and 58 mole% Thallium Iodide) which has a high refractive index and high polish, but the disadvantages of solubility in base and toxicity. Silver Chloride, although commonly used in ATR in prisms and pressed plates, is soft, pliable and easily deformed under pressure, and discolours in visible light. Germanium

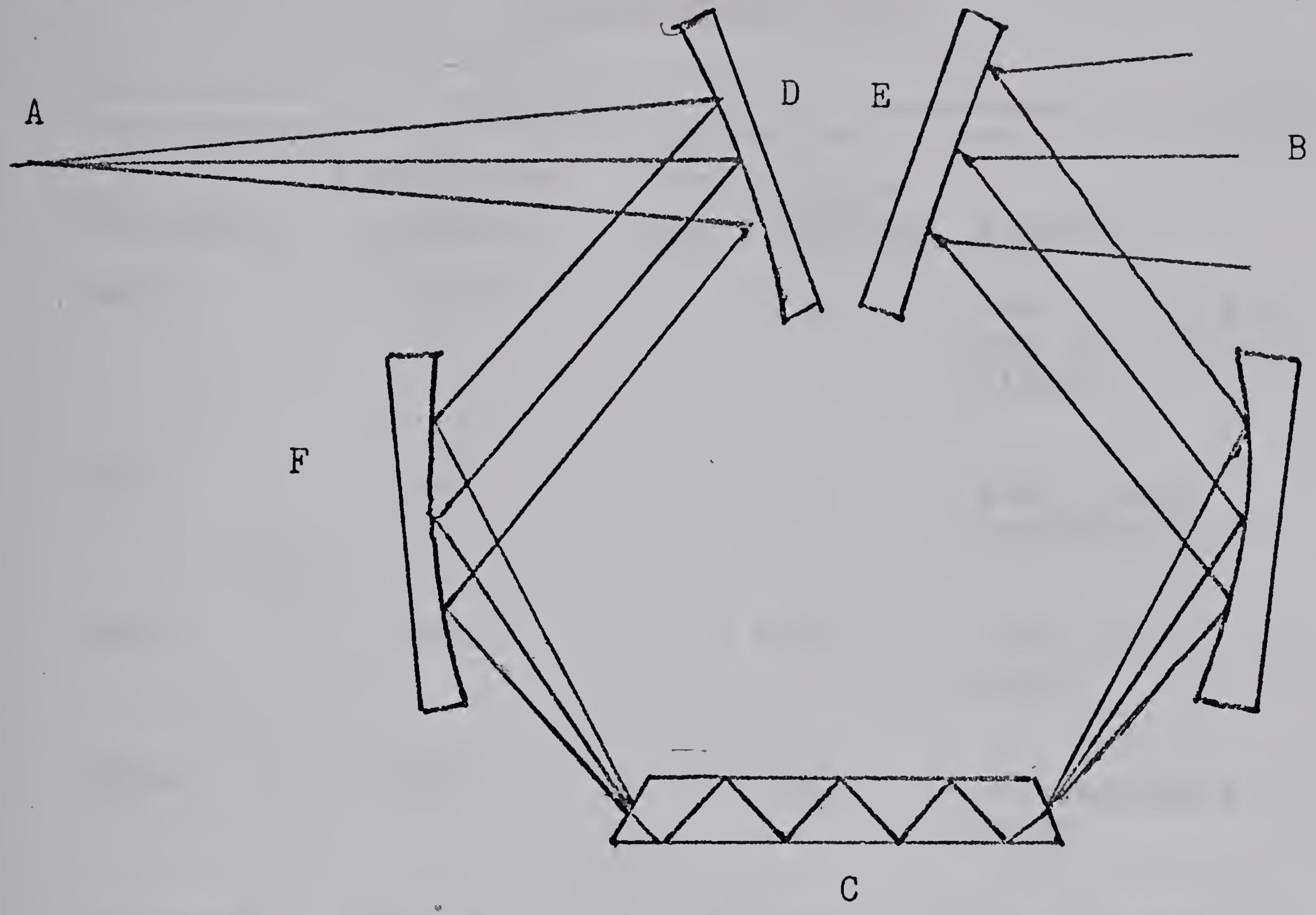

Figure 6. Schematic diagram of FMIR optical system. A, entrance slit of spectrophotometer; B, source; C FMIR prism plate; D, E, F, G, adjustable mirrors.

TABLE V. PROPERTIES OF PRISM MATERIALS FOR REFLECTANCE SPECTROSCOPY (5-a)

Material	Refractive Index	Transmission Range, microns	Comments
NaCl	1.519	1 - 16	low n, brittle, use for organic liquids
CsBr	1.667	1 - 36	long range transmission
AgCl	1.997	2 - 22	soft, discolours easily
KRS-6	2.192	2 - 20	intermediate n, tough
Irtran-2	2.245	2 - 13	very durable
KRS-5	2.380	2 - 35	most useful, toxic, soluble in base.
Ge	4.017	2.5 - 15	highest index

is especially good for samples loaded with free Carbon. KRS-6 (40 mole % Thallium Bromide and 60 mole % Thallium Chloride) is extremely useful for a long wavelength range. Irtran-2 has good physical characteristics, i.e., high refractive index, inertness, opaque up to 125°C, but gas high reflection losses and is only useful in a short range - up to eleven microns.

Since ATR deals with a single reflection, large penetration is desired and the prism material refractive index should be fairly low. This is shown as n_{p1} in fig. 4. Unfortunately, use of materials with a lower refractive index (such as AgCl) results in some distortion of the reflectance band at higher wavelengths. (fig.5) This distortion is not found in FMIR because of the multiple reflections which then require less penetration per reflection, allowing a prism material of higher refractive index to be used. Normally a material with refractive index of level n_{p3} in fig. 4 is used.

Spectral distortion can also occur when the angle of incidence on the reflecting surface approaches or exceeds the critical angle whose sine is expressed as n_r/n_d (or in terms of prism and sample n_s/n_p). Thus for a given prism material and fixed angle of incidence caution must be used in the choice of sample material and its associated

refractive index. At a fixed angle of incidence for a given crystal there is a critical index above which total reflection ceases. That is to say, the critical index occurs when the angle of incidence equals the critical angle of the system. To reduce spectral distortion, a safe index is defined as being the index of refraction 0.2 units below the critical index (24). For example with KRS-5 (refractive index 2.4) the critical index for the rarer medium at angle of incidence 30° equals $2.4 \times \sin 30^{\circ} = 1.2$. The safe index is then placed at 1.0. Values for critical and safe indices are given for KRS-5, AgCl and Ge for various angles of incidence in Table V1.

Reflection spectra are not identical to transmission spectra but are similar and provide valuable spectroscopic information of otherwise intractable samples such as adhesives, rubbers, fabrics and crystals (5-b, 26). Sampling is simple, the only criterion being the availability of a smooth surface, and the results are independent of sampling thickness.

Since in reflectance spectroscopy, particularly in FMIR, only one surface of the sample need be in contact with the prism-plate to provide a good spectrum, it is possible to leave the other surface open to the air or to any cell applicable to the desired experiment. This

TABLE V1. CRITICAL AND SAFE INDICES FOR KRS-5, AgCl, AND GERMANIUM (24)

Material	Angle of Incidence	Critical Index	Safe Index
KRS-5 (n = 2.4)	30°	1.25	1.05
	45°	1.7	1.5
	60°	2.0	1.8
AgCl (n = 2.0)	30°	1.0	0.8
	45°	1.4	1.2
	60°	1.7	1.5
Germanium (n = 4)	30°	2.0	1.8
	45°	2.8	2.6
	60°	3.5	3.3

property makes it practicable to the diffusion experiment. In this experiment a film of constant thickness of "solvent" can be placed on the surface of the prism-plate and then covered with a cell system which will provide a constant flow of "solute". If the film is of considerable thickness relative to the penetration depth of the beam power, then as diffusion takes place, the change of concentration at the plate surface (or h/2 of the theoretical slab) can be measured continuously by measuring the change in absorption at a fixed wavelength. By choosing a viscous solvent such as found in liquid phases in gas chromatography, and by feeding the solute as a vapour in a carrier gas, a gas chromatographic situation is approximated. The change of concentration with time is measured and from this the diffusion coefficient can be calculated, and information allowing elucidation of the liquid phase mass transfer term can be obtained.

For maximum workability of this method, it remains to be seen whether absorbance values found by FMIR need to be transformed into concentration values, or if the absorbance plots can be used directly in evaluating the diffusion coefficient. Since the spectrophotometer used in this work records on a linear percent transmittance scale, it is preferable to replot the original spectra on a linear absorbance scale. Assuming Beer's law ($A = abc$) to be valid,

the slope of the plot at any time t can be expressed as $\Delta A/\Delta t = ab\,\Delta c/\Delta t$, where, for the system ab remains constant. Taking the logarithms of these various slopes the expressions become $\log ab + \log(\Delta c/\Delta t)$. If these values are plotted and the slope of the resulting straight line taken, the expression for the slope will be $\Delta\log(\Delta c/\Delta t)/\Delta t$, which in the limit would be $\Delta\log(dc/dt)/\Delta t$. This in turn is the slope of the straight line expected from equation (xv) page 13 . Thus, no transformation of values from absorbance to concentrations need be made and the diffusion coefficients can be calculated almost directly from the spectra.

11 EXPERIMENTAL

11 - 1 Reagents

The reagents used in the experimental work as solvents (layer materials) were: Fluorolube S-30 (Hooker Electrochemical Company), Carbowax 600, Carbowax 1500, Dinonylphthalate (DNP), D-C Silicone grease, and Ucon 50-HB 280X (all from F & M Scientific Company). The samples chosen were 1-pentene (Fisher technical grade), 2-methyl butane (isopentane Phillips 66 commercial) diethyl ether (Malinckrodt anhydrous) and wash acetone. The Beer's law plots (figs. 13 & 14) were made using dodecane (Matheson, Coleman

and Bell).

11 - 2 Design of Apparatus

A Perkin-Elmer IR-137-Infracord- with a Wilks Model 12 MIR attachment and KRS-5 plates was used. The Infracord was equipped with an outlet to an external recorder (Sargent Model SR variable speed). By use of a 10 millivolt plug the scale was expanded so that 0-100 per cent transmittance used full recorder scale.

In order to use thin films of constant thickness in FMIR it was necessary to have the plates in a horizontal position. Since in normal use the plates are placed vertically, it was decided to turn the Infracord on its side. A dexion support was bolted to the Infracord as shown in fig. 7 and the spectrophotometer was turned, braced with wood and wired to the wall. The dexion allowed the controls to be manipulated. When operated in this position, the Infracord did not show any serious effects with respect to scan, gain, wavelength shift, but did show some heating effects due to the alignment of the source, and some misalignment of the mirrors causing the beam to be shifted slightly. The mirrors were adjusted and to counteract the heating effects, the machine was turned off and allowed to cool every two or three hours.

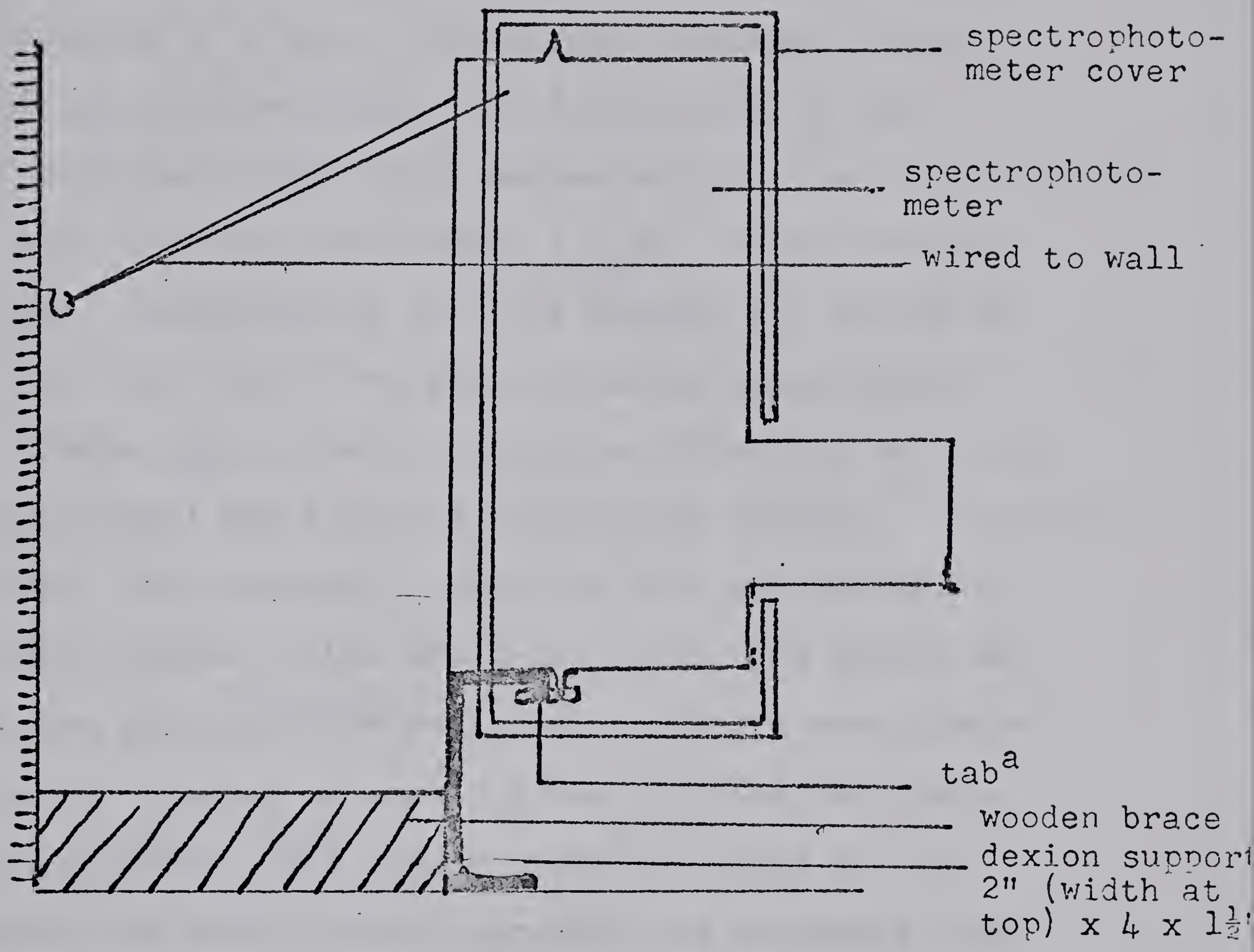

Figure 7. Schematic diagram of the spectrophotometer as supported on its side.

a. Tabs are welded to the dexion at intervals determined by the bolts in the ledge on the spectrophotometer. Holes are bored in these tabs and the dexion is bolted to the spectrophotometer through the tabs.

Two cell covers, CC-A and CC-B (see figs. 8, 9, 10) were designed for the FMIR solid sampling cell to provide for the analysis of a layer of constant thickness and for passage of gas over the layer. CC-A consisted of two pieces of stainless steel which supported the prism-plate on both sides but left about 1.4 cm. of open surface between them. Enough space was left between the bottom of the cover and the top of the plate to allow insertion of spacers. These spacers were constructed from shim materials of stainless steel and brass of thicknesses 0.005cm. - 0.023 cm. (127 microns - 584 microns). When the cell was assembled, the plate was placed on the solid-cell base, the spacer was placed on the plate and the cell covers in turn were placed on the spacer, leaving an area 3.4 cm. x 1.2 cm. of plate open to the surface. The liquid could be spread on the open surface and with a teflon spreader its thickness regulated to that of the spacer. In all runs a layer of KEL-F #90 (halofluorocarbon) grease was smeared on the bottom of the spacer to give a better seal between the spacer and the plate without interfering with the absorption measurements.

CC-B was constructed from a single piece of steel 4.5 cm. x 3.7 cm. x 1 cm. with a cavity 1.2 cm. x 3.4 cm. x 0.8 cm. designed to fit exactly over the part of the plate exposed by the spacer. Two holes were drilled from the top of the cell

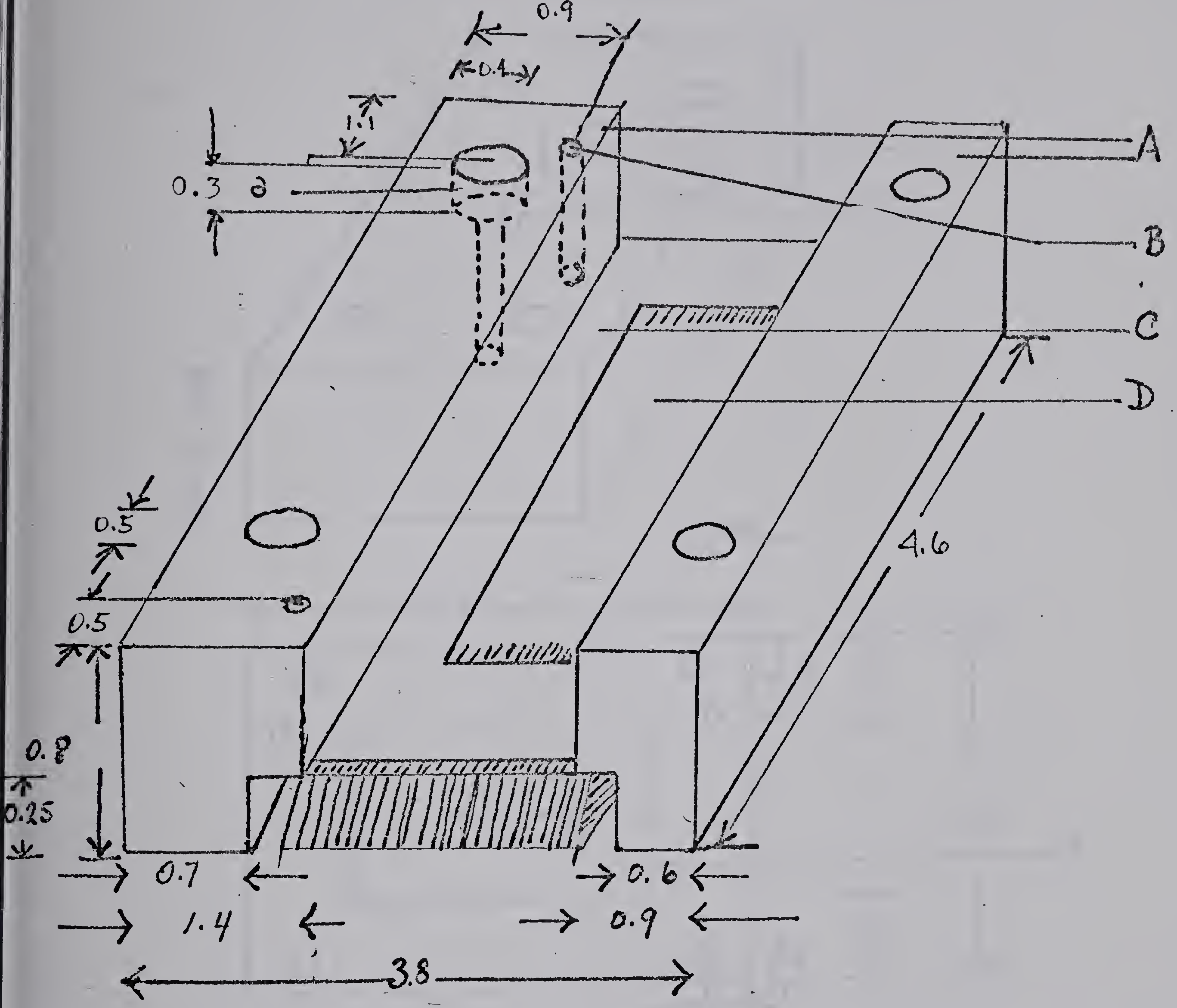

Figure 8. Schematic diagram of cell cover CC-A designed for FMIR solid sampling cell: A - two pieces of stainless steel, B - holes drilled for solid cell (diameter 0.3 cm), C - spacer, D - FMIR prism plate. All measurements are given in cm.

a. Holes at four corners all drilled as shown in diagram.

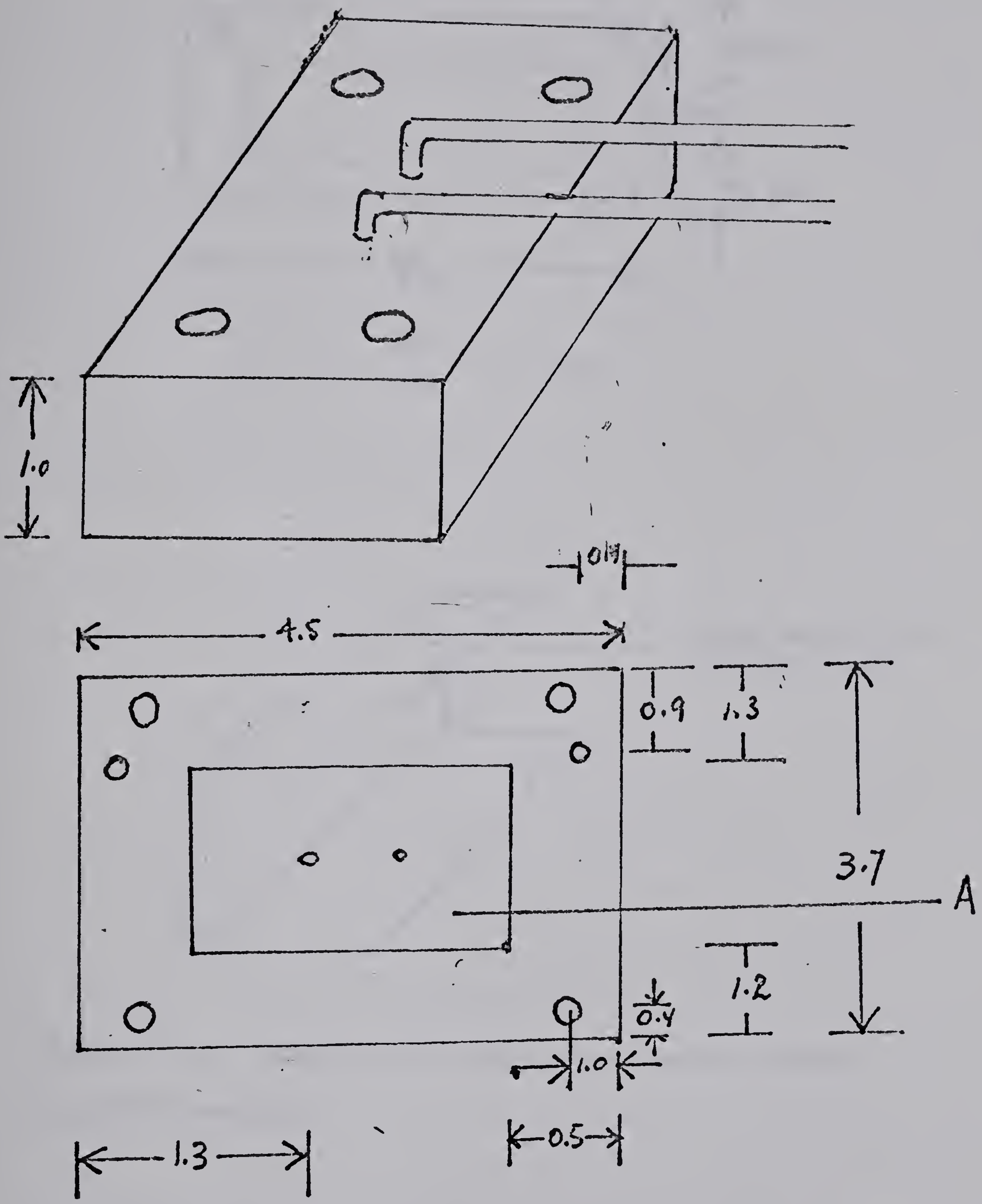

Figure 9. Schematic Diagram cell cover CC-B exterior and bottom view: A - cavity 0.8 cm deep. All dimensions in cm. The holes are drilled as in figure 8.

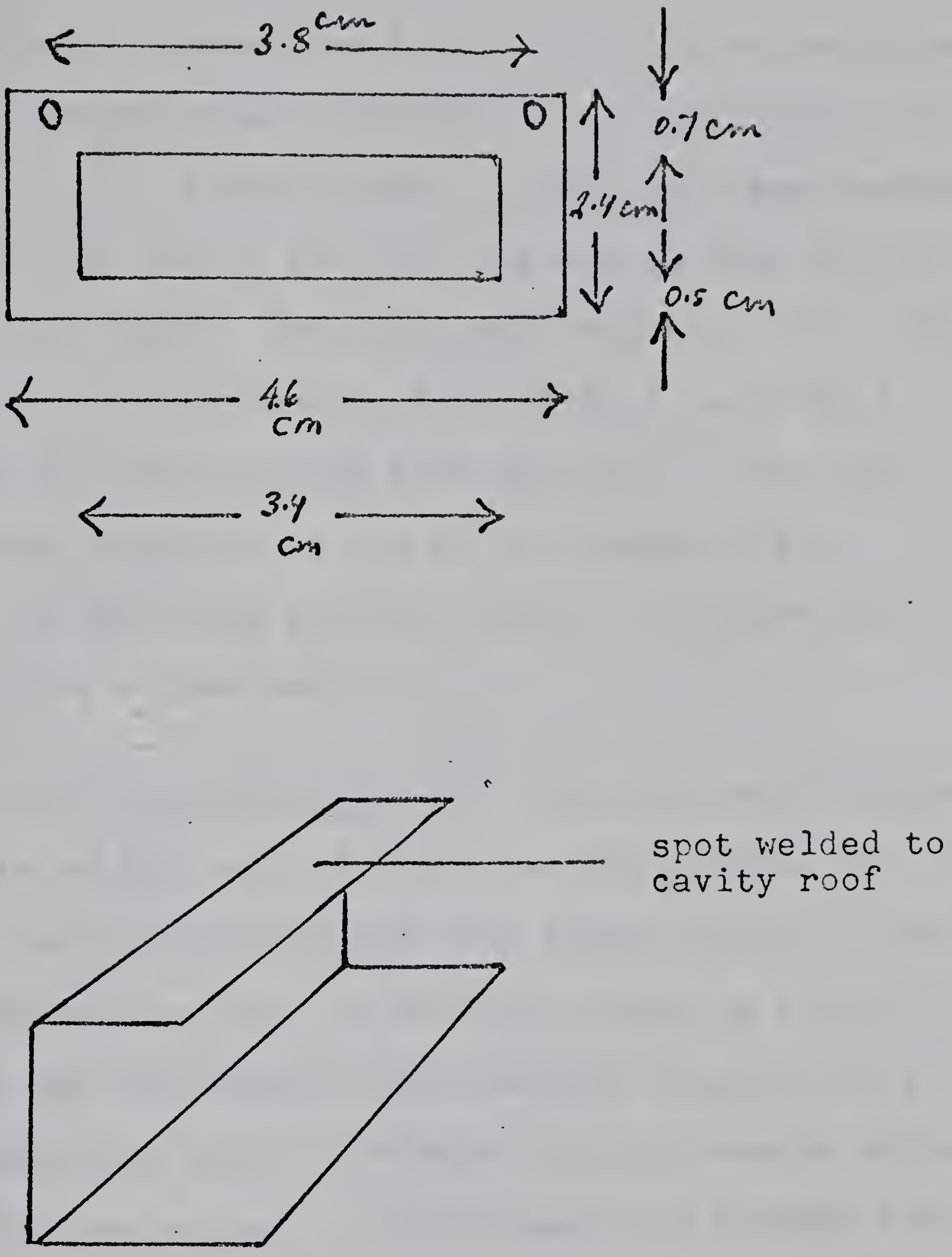

Figure 10. Spacer, top view, and baffle system for CC-B cavity.

into the cavity and these were fitted with 0.2 cm. stainless steel tubing sections which extended 15 cm. beyond the cell and parallel to it. A small piece of metal was spot welded to the roof of the cavity and this was bent so that it extended across the cavity about 0.3 cm. from its roof. This "baffle" prevented disturbance of the liquid layer by a direct jet of the incoming gas (see fig. 10). This cell cover was placed directly on top of the spacer and a second layer of KEL-F was applied between the spacer and the cover to give a good seal.

A system utilizing two four-way stopcocks was designed to feed sample to the cell (CC-B), i.e., to provide flow of pure carrier gas and carrier gas plus sample vapour (see fig. 11). The carrier gas was bubbled through a fritted glass bubbler and the sample saturator was immersed in a constant temperature bath to provide constant sample vapour pressure. This system kept a continuous flow through the sample preventing pressure build-up in the flask and resultant "explosion" of sample vapour in the system when it was changed from carrier gas to sample flow.

The system from the bubbler to the cell was made basically of 0.4 cm. glass tubing with joints of tygon. The steel tubing of the cell was inserted into the glass tubing and the joint sealed with black wax. The cell was attached to and dismantled from the system at the first

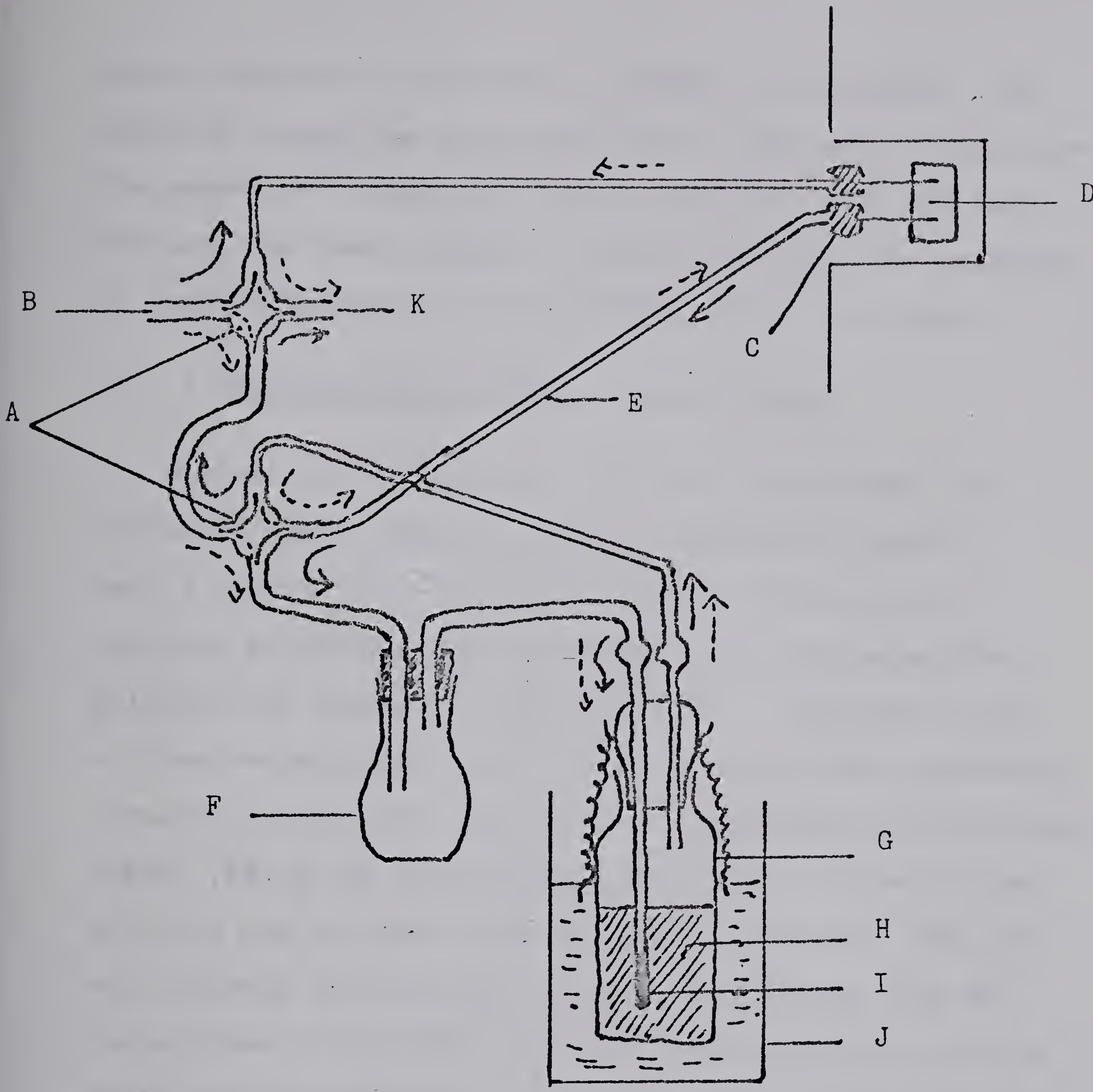

Figure 11. Sampling system. A, four-way stopcocks; B, Helium inlet; C, black wax seal; D, cell with CC-B; E, 4mm glass tubing; F, trap; G, bubbling jar (saturator); H, sample; 1, fritted glass bubbler; J, constant temperature water bath, K, outlet for waste gas.

The solid arrows correspond to pure carrier gas flow through the system: the dashed arrows correspond to the sample flow through the system.

tygon connection so as not to disturb the wax seal. The sampling system was positioned near to the cell to minimize the amount of tubing required to reach the cell and thus decrease the dead volume of the cell and the time required to reach saturation of sample vapour above the layer.

11 - 3 Verification of Beer's Law for FMIR

Before proceeding with the actual measurement of diffusion coefficients it seemed necessary to verify Beer's law for this particular system; studies of absorption at various concentrations were made using CC-A. Solutions of dodecane (vapour pressure - less than 1 mm. at room temperature) (4) in fluorolube at known concentrations were prepared. The cell was assembled with 254 micron spacer (KEL-F #90 grease seal) and a smooth layer of the solution was applied using the teflon spreader. The cell was inserted in the spectrophotometer sampling area and the mirrors of the FMIR attachment were adjusted to focus maximum beam energy on the entrance slit of the Infracord -- it was found necessary to do this frequently as the slightest movement of the mirrors could cause a serious energy loss. The wavelength was scanned from 3.0 to 4.0 microns (see fig. 12). Since fluorolube does not absorb in this region, it was not necessary to use fluorolube on the reference plate. The resulting peak at about 3.4 microns (alkane C-H

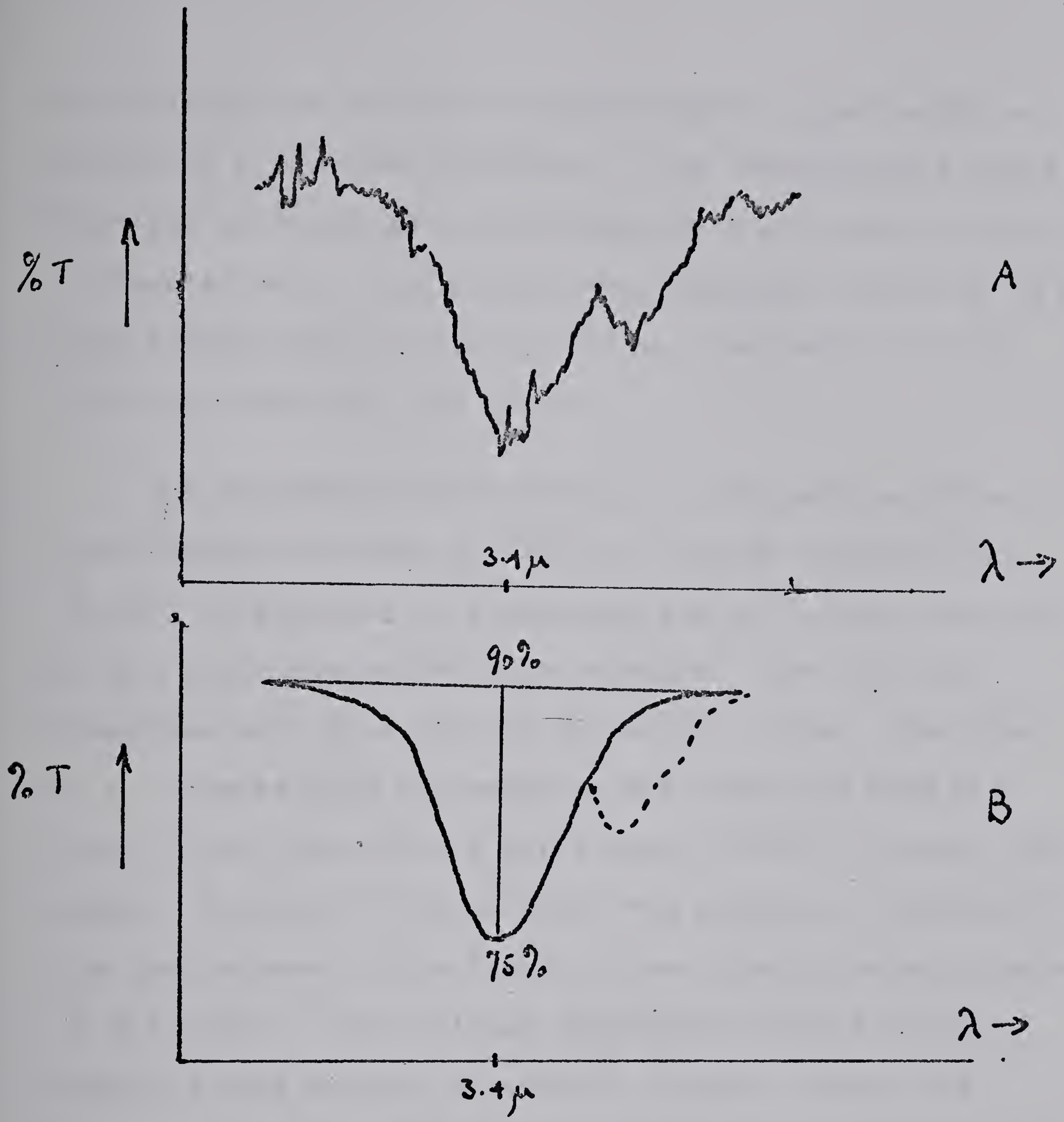

Figure 12. Spectrum analysis for calculation of Beer's Law plot. Spectrum of 0.35M solution of dodecane in fluorolube. A, spectrum as it appeared; B, spectrum as analyzed for peak height, ΔA.

[illegible]

stretching) was analyzed by measuring the peak height at the point of maximum absorption. The transmittance units from the spectrum were transformed into absorbance units by Beer's law $A = \log 1/T$ and the resultant values of ΔA were plotted against concentration. For data and plot refer to Table V11 and fig. 13.

The dependence of absorption on the path length was investigated by using a solution of known concentration (0.26M) of dodecane in fluorolube and by varying the area of the plate covered by this solution. The cell was assembled with CC-A and the 254 micron spacer. The area to be covered with the solution was separated from the rest of the plate with a thick smear of KEL-F across the plate. A layer of the solution was placed on one side of the grease smear and a layer of pure fluorolube was placed on the other. The cell was immediately placed in the sampling area and the wavelength scanned - speed was necessary in order to avoid mixing of solutions across the grease barrier. This procedure was repeated for several coverages, i.e., 7mm, 10mm, 21mm, 25 mm, and 34mm. The spectra were analyzed in the same manner as before and the resultant absorption data were plotted against the effective coverage. The results are shown in Table V111 and fig. 14 .

11 - 4 Measurement of Diffusion Coefficients

For the measurements of diffusion coefficients the

TABLE V11. ABSORPTION AT 3.4 MICRONS OF SOLUTIONS OF DODECANE IN FLUOROLUBE AT VARIOUS CONCENTRATIONS

Solution	Concentration	Δ A
A	0.09 M	0.026
B	0.13 M	0.035
C	0.15 M	0.036
D	0.17 M	0.046
E	0.20 M	0.051
F	0.22 M	0.049
G	0.24 M	0.060
H	0.26 M	0.059
I	0.31 M	0.075
J	0.35 M	0.084
K	0.40 M	0.090
L	0.44 M	0.103

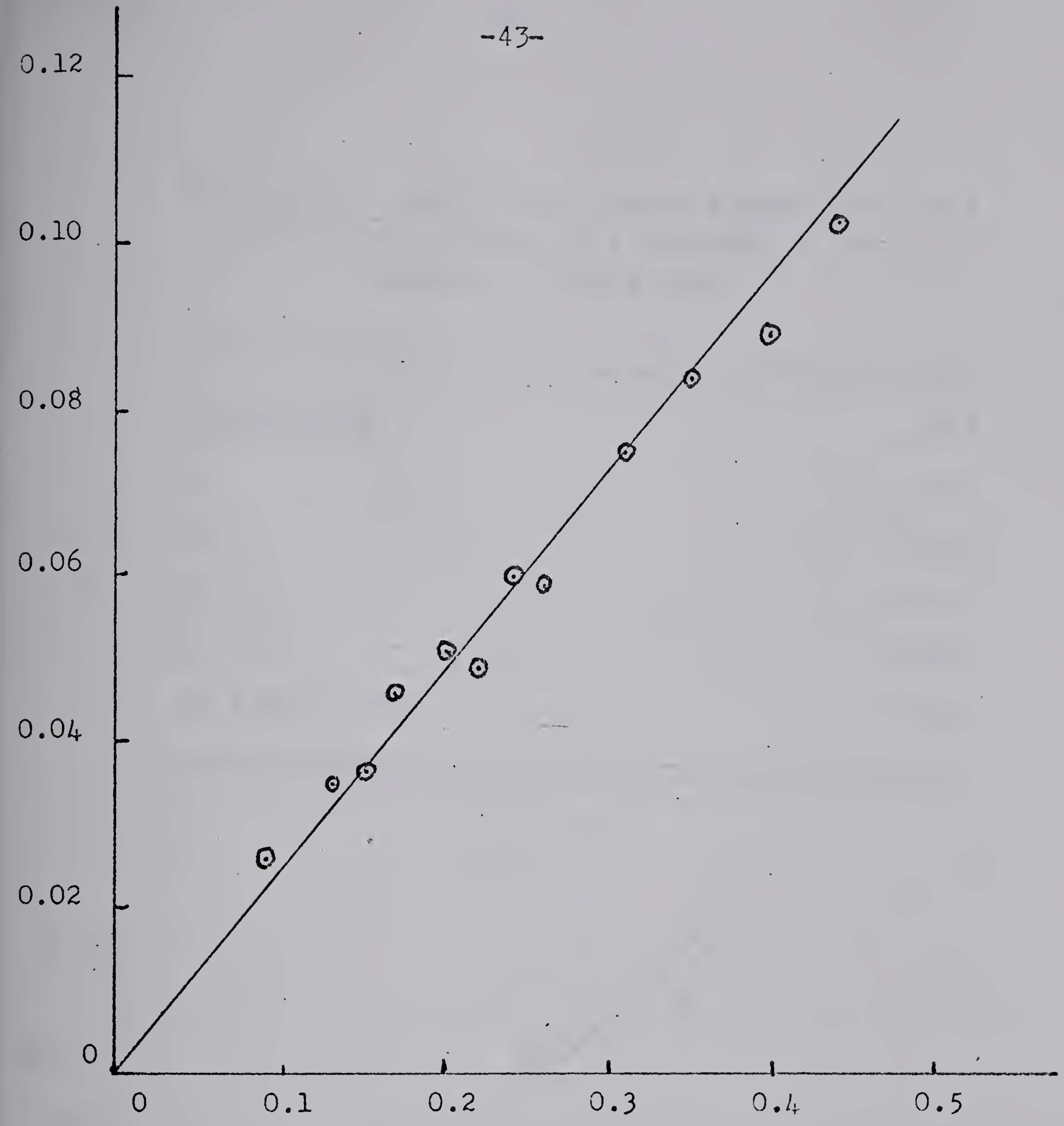

Figure 13. Beer's Law plot, Absorbance versus concentration, for solutions of dodecane in fluorolube (Data from Table V111)

TABLE V111. ABSORPTION AT 3.4 MICRONS OF 0.26 M SOLUTION OF DODECANE IN FLUOROLUBE AT VARIOUS COVERAGES OF FMIR PLATE

Coverage, mm	ΔA
7	0.013
10	0.020
21	0.035
25	0.048
34 (full plate)	0.056

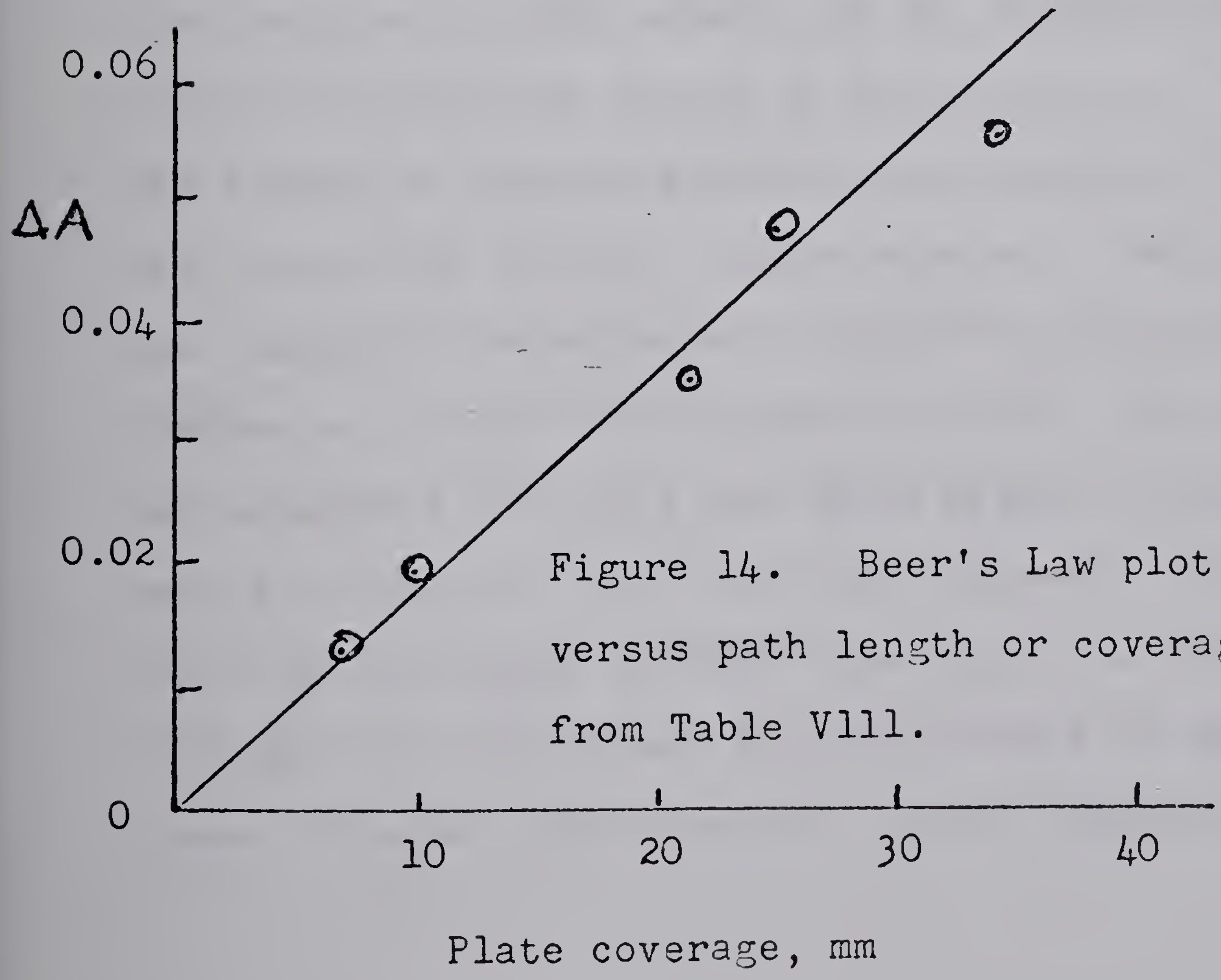

Figure 14. Beer's Law plot of absorption versus path length or coverage of the plate--from Table V111.

solute-solvent systems were chosen on the basis of favorable physical and spectroscopic properties. The solute samples were chosen on the basis of vapour pressure - of the order of 400 - 600 mmH_g. The samples chosen were 1-pentene (vapour pressure: 100 mm at -28.0°C, 400mm at 12.8°, and 760mm at 30.1°), 2-methylbutane (v.p.: 100mm at -20.2°, 400mm at 10.5°, and 760mm at 27.8°) and diethyl ether (v.p.: 100 mm at -11.5°, 400mm at 17.9° and 760mm at 34.6°) (4). The liquid layer (solvent) was chosen to be fluorolube because of the lack of absorption bands in the region 3 - 7 microns.

The wavelength of maximum absorption for alkane C-H stretching (about 3.4 microns) was determined by scanning the spectrum of pure solute and the spectrophotometer wavelength drum was locked in that position. The sample was placed in the gas bubbling jar (saturator) at a level well above the fritted glass bubbler. The bubbling jar was placed in the constant temperature water bath and the thermostat on the bath was set for 20°C. The FMIR cell was assembled with CC-A and using spacer of desired thickness the layer of fluorolube was prepared. After removing CC-A, an even layer of KEL-F was spread on the bottom of CC-B and this cell cover was then placed on the spacer and plate. The cell was inserted in the spectrophotometer and

the inlet and exit tubes were connected to the sampling system at the tygon joints. The carrier gas, Helium, was allowed to flow through the system with flow rate 0.55 ml/sec. With pure carrier gas in the system the recorder was turned on and the time scan begun to establish a base-line. After a short time both stopcocks were turned simultaneously to start sample flow and this point was recorded on the chart paper as zero time. Recording speed for most runs was set at "fast" or five inches per minute. When equilibrium concentration was reached in the layer (when there was no further change in absorbance) the stopcocks were again turned and the system cleared of the solute. The flow through the cell was then cut off, the cell dismantled, cleaned with chloroform, and the run repeated. For each of the three samples forty runs were made, ten for each spacer (four spacers of thicknesses 127μ, 254μ, 381μ, and 584μ were used).

To examine the effect of solvent (liquid layer) on the diffusion coefficients, experiments were carried out using D-C Silicone grease (F & M Scientific Co.), Carbowax 600, Carbowax 1500, Dinonylphthalate, and Ucon -50-HB 280x-all F & M Scientific Co. products). Infrared spectra of these liquids were taken and compared to find a common region of no absorption. With the exception of dinonylphthalate these liquids showed no absorption in the region

4 - 6 microns ($2500 cm^{-1}$ - $1650 cm^{-1}$). Dinonylphthalate had an absorption band (C=O stretching) at about $1730 cm^{-1}$. It was decided to use acetone as the sample and its band at about $1750 cm^{-1}$ to monitor the change in concentration. In the acetone-dinonylphthalate system, the slight difference in position of peak maxima allowed the change of concentration to be followed although the energy of the beam was seriously reduced by the absorption of DNP. Using only the 127 micron spacer for the very viscous solvents - Carbowax 1500, D-C silicone grease - and both 127 and 381 micron spacers for DNP, Ucon and Carbowax 600 (because of their lower viscosity) the procedure mentioned above was repeated with the wavelength selector locked at 5.75 microns, and the resulting spectra were analyzed.

11-5 Comparison of the Rate of Sample Delivery to the Surface with Rate of Diffusion into the Liquid

The rate of delivery of sample to the surface of the layer must be large compared to the rate of diffusion into the liquid for the diffusion data obtained to be valid, i.e., concentration of solute above the plate must be constant. This was tested by measuring the amount of solute present in the film at equilibrium concentration as a fraction of the solute that passed through the cell cavity during the time taken for the layer to achieve

equilibrium concentration.

For the samples of higher vapour pressure, 1-pentene, 2-methylbutane, diethyl ether, 1-pentene was used in showing that the rate of depletion of sample vapour from the cavity is in fact small enough to justify the assumption that the amount of sample above the layer remained constant.

Values of vapour pressure of 1-pentene were plotted (fig. 15) at several temperatures and the value of vapour pressure at 20°C was obtained from the resulting curve - 550 mm Hg.

The cell was assembled with CC-A and the 254 micron spacer; a layer of fluorolube was applied to the plate. With 1-pentene in the bubbling jar, the water bath temperature set at 20°C, the flow rate at 0.34 ml/sec, and the wavelength selector of the spectrophotometer locked at 3.4 microns, the cell cover CC-B was placed on plate and the procedure for measuring diffusion coefficients was followed. The point corresponding to the time at which equilibrium concentration in the layer was reached was marked on the resulting spectrum, i.e., 53 sec. The ΔA at this point was calculated and from the Beer's law plot for dodecane in fluorolube the equilibrium concentration was estimated. The value of ΔA, 0.05 absorption units, corresponded to

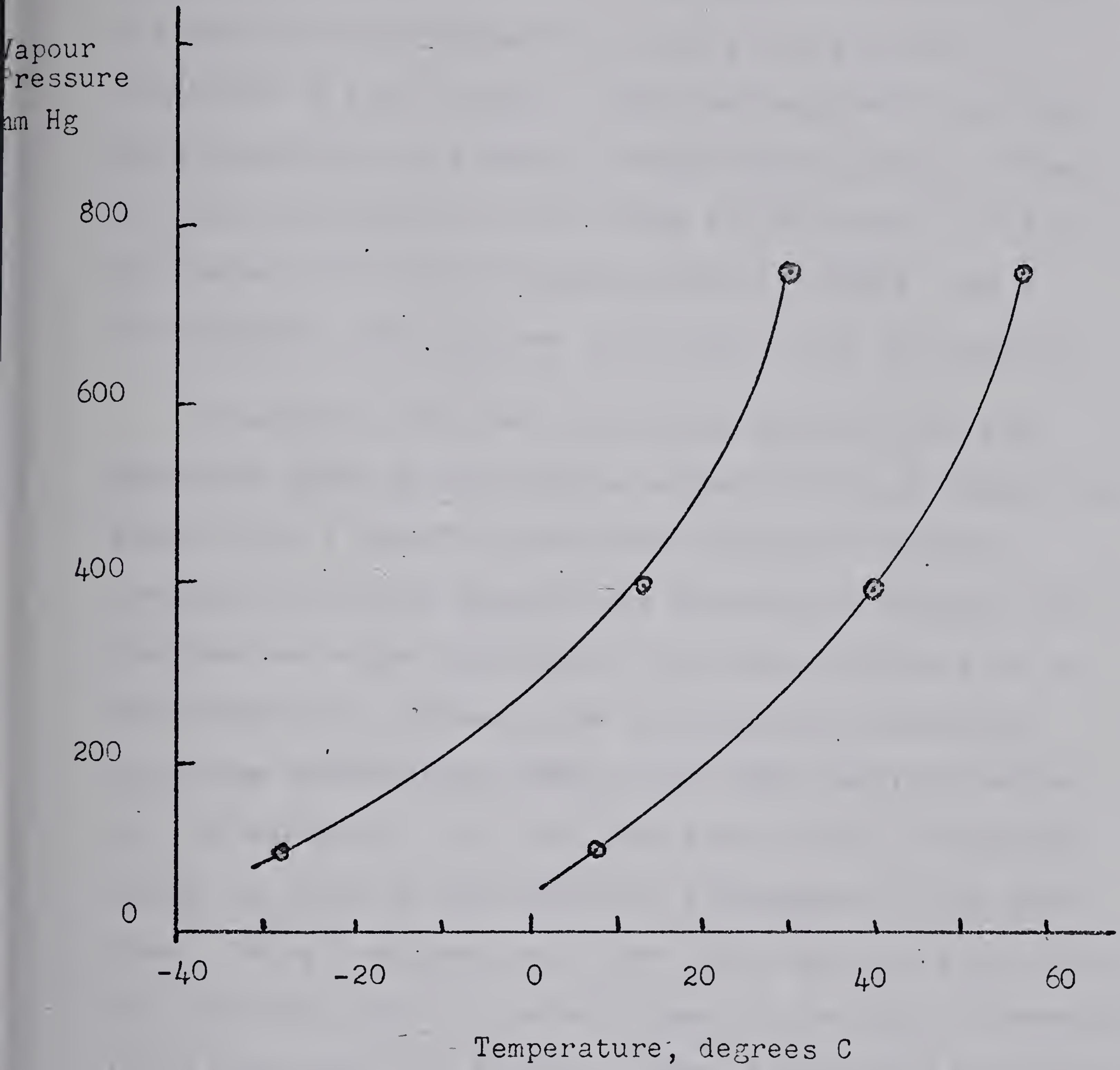

Figure 15. Vapour pressure curves for 1-pentene and acetone.

concentration value of 0.2M. The amount of 1-petene in the layer was calculated to be 1.2 x 3.4 x 0.0254 x 0.2/1000 = 2 x 10^{-5} moles. The time required to deliver this amount into the sample cavity was calculated. From the ideal gas law PV = nRT, where P = 0.73 atm, n = 2 x 10^{-5} moles, R = 0.08 1 atm/deg mole, T = 293°A, and V = (0.34/1000)t, the time was calculated to be two seconds.

In any run there will be a time required for the system to reach an equilibrium concentration of sample and since this is related to the dead volume of the cell (volume of delivery system from stopcock to cavity) this time can be called dead-time. The value of this time can be estimated by following the procedure for measuring diffusion coefficients using a very thin layer of solvent (5 - 10 microns). The time from zero to time of initial change as shown on the spectrum is designated to be dead-time. Using 1-pentene and a very thin layer of fluorolube the dead-time for the system is seen to be about 15 seconds (with flow rate 0.34 ml/sec). Thus, taking this time into consideration, the time for the layer to reach concentration of 0.2M is considered to be 53-15 = 38 seconds. The time taken to allow 2 x 10^{-5} moles of 1-pentene to pass through the cell is only a fraction of the time during which the layer has equilibrium concentration of solute above it, 2/38 = 5%; and from this it is concluded that the rate of

depletion from the cell cavity is much less than the rate of sample delivery to the cell, and that the diffusion data obtained is valid for the 1-pentene--fluorolube system. Because of the similarity of vapour pressures of 2-methylbutane and diethyl ether to that of 1-pentene, these conclusions can be extended to these systems..

There was some doubt about using acetone as a sample, since it has a low vapour pressure compared to the compounds mentioned above (100mm at 7.7°, 400mm at 39.5° and 760mm at 56.5°) (4). With low vapour pressures it seemed possible that the rate of delivery might be reduced and that the rate of depletion might become large enough to affect the diffusion data. Calculations similar to those done for the 1-pentene--fluorolube system were done for the acetone--Carbowax 600 system.

Solutions of acetone in Carbowax 600 in known concentrations were prepared (Table 1X). The cell was assembled with CC-A and the 254 micron spacer and a layer of the solution was applied. The cell was inserted in the spectrophotometer and the wavelength was scanned from 5 - 6 microns. The peak height at about 5.75 microns (maximum wavelength for C=O stretching in ketones) was measured and the resulting ΔA value was calculated for each solution. A Beer's law plot of ΔA versus concentration was made

TABLE 1X. ABSORPTION AT 5.75 MICRONS OF SOLUTIONS OF ACETONE IN CARBOWAX 600 AT VARIOUS CONCENTRATIONS

Solution	Concentration	ΔA
A	0.35 M	0.065
B	0.60 M	0.12
C	0.80 M	0.15

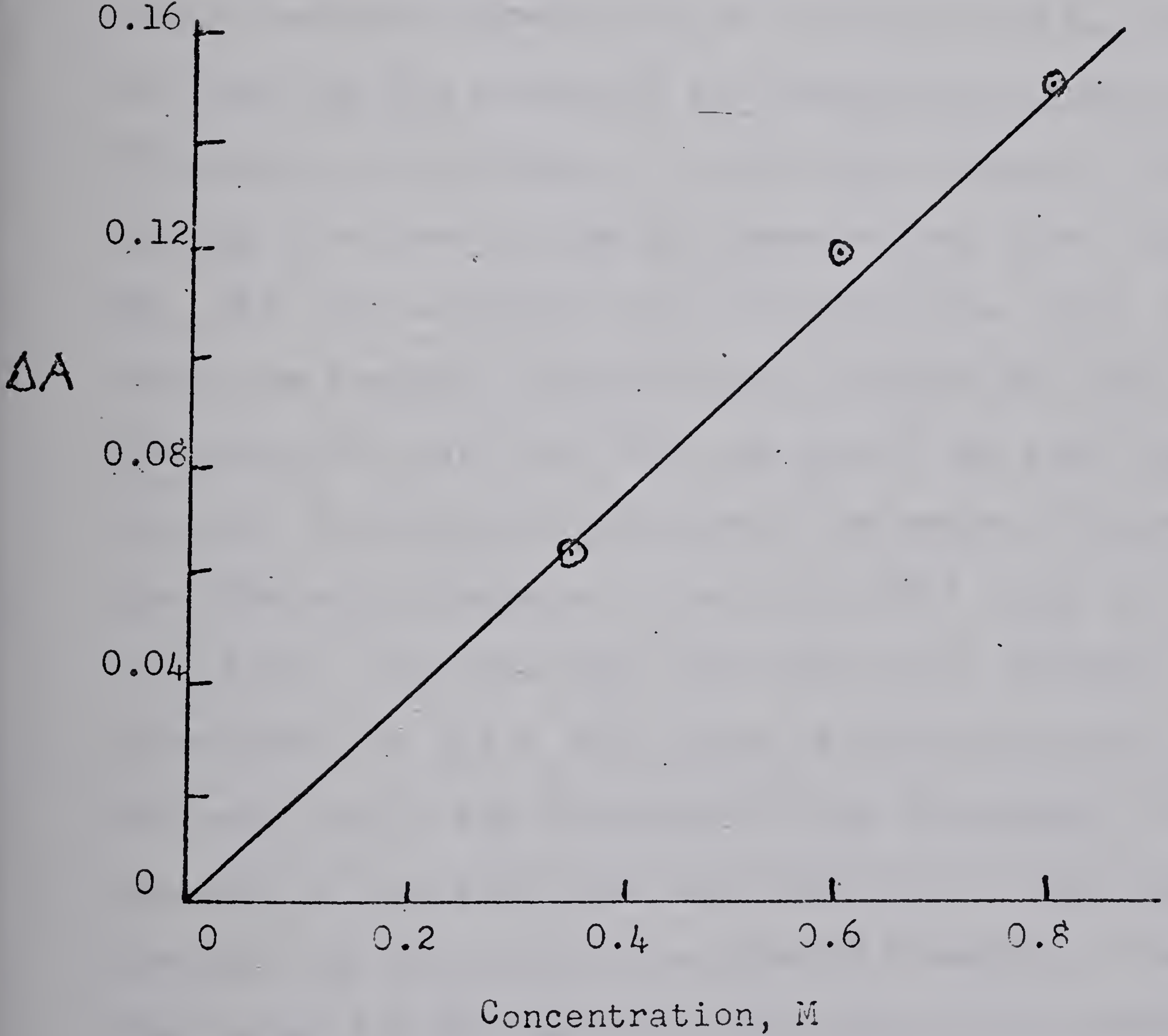

Figure 16. Beer's Law plot, absorbance versus concentration for solutions of acetone in carbowax 600 (Data from Table 1X)

(fig. 16) and the line drawn.

Values of vapour pressures of acetone were plotted at several temperatures (fig. 15) and the value at room temperature ($\sim 25^{o}$C) was taken from the curve.

The cell was assembled with CC-A and 127 micron spacer and a layer of Carbowax 600 was applied. With acetone as sample, the water bath temperature at 25^{o}, flow rate at 0.55 ml/sec, the spectrophotometer wavelength selector locked at 5.75 microns, CC-B was placed on plate and the procedure for measuring diffusion coefficients was followed. A point was chosen on the resulting spectrum at time 216 seconds from zero time. The ΔA was calculated, and assuming this value represents the average concentration of solute in layer, the concentration was read from the Beer's law plot (fig. 16). From the dimensions of the layer the amount of acetone in the film was calculated to be 1.7×10^{-4} moles ($A \simeq 0.62$, $c \simeq 3.2$ M). From the flow rate and vapour pressure the time taken for 1.7×10^{-4} moles of solute to pass through the cell cavity was calculated to be 22 seconds. An estimate of the dead-time was made using a thin layer of Carbowax 600 and found to be about 18 seconds. The time then taken for the layer to reach equilibrium concentration 3.21 M was approximately $216 - 18 \simeq 198$ seconds: the time

taken to allow 1.7 x 10^{-4} moles of acetone to pass through the system was about 11% of this time. From this it was concluded that for the acetone--Carbowax 600 system a constant concentration of acetone is maintained above the layer. This conclusion was assumed to cover the acetone systems as well.

111 RESULTS AND DISCUSSION

111 - 1 Experimental Results

The spectra were analyzed by replotting the per cent transmittance data as absorption data and the best curves were drawn. To each of the curves tangents were drawn at several points and the slopes of these tangents were measured. The logarithms of the slopes were taken and for each curve a plot of log slope against time was made. The best straight line through these points was drawn and the slope measured. From equation (xv) it is seen that the slope of this line is equal to $-\pi^2 D/ 2.3\ h^2$, and thus from the slope the diffusion coefficient can be calculated.

Examples of the original spectra (figs. 17,18, and 19), are replotted in figures 20, 21 and 22 from transmittance values to absorbance values. On these plots tangents are drawn and the logarithms of the slopes for these examples

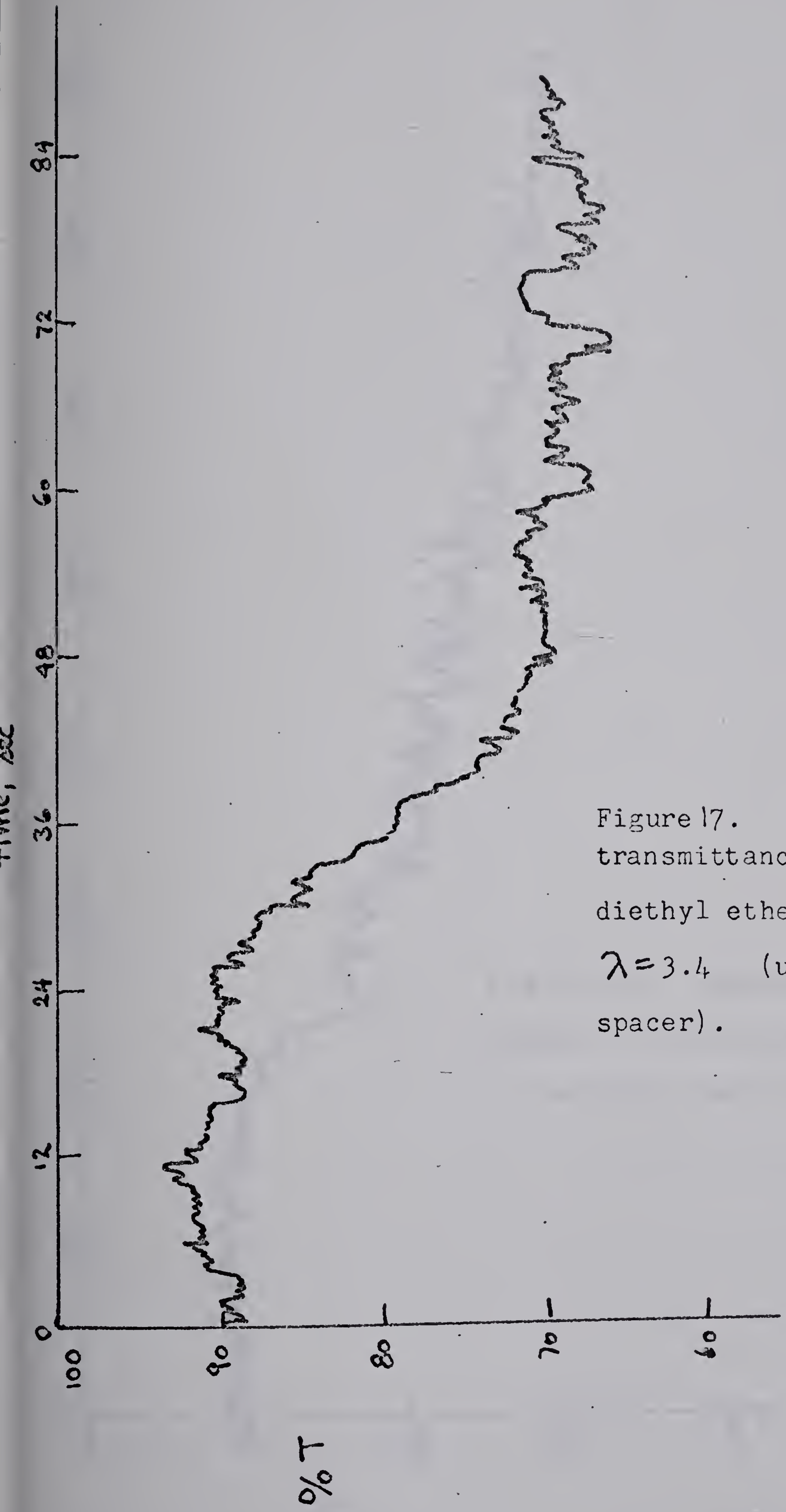

Figure 17. Spectrum (percent transmittance versus time) of diethyl ether in fluorolube at $\lambda = 3.4$ (using CC-B, 254μ spacer).

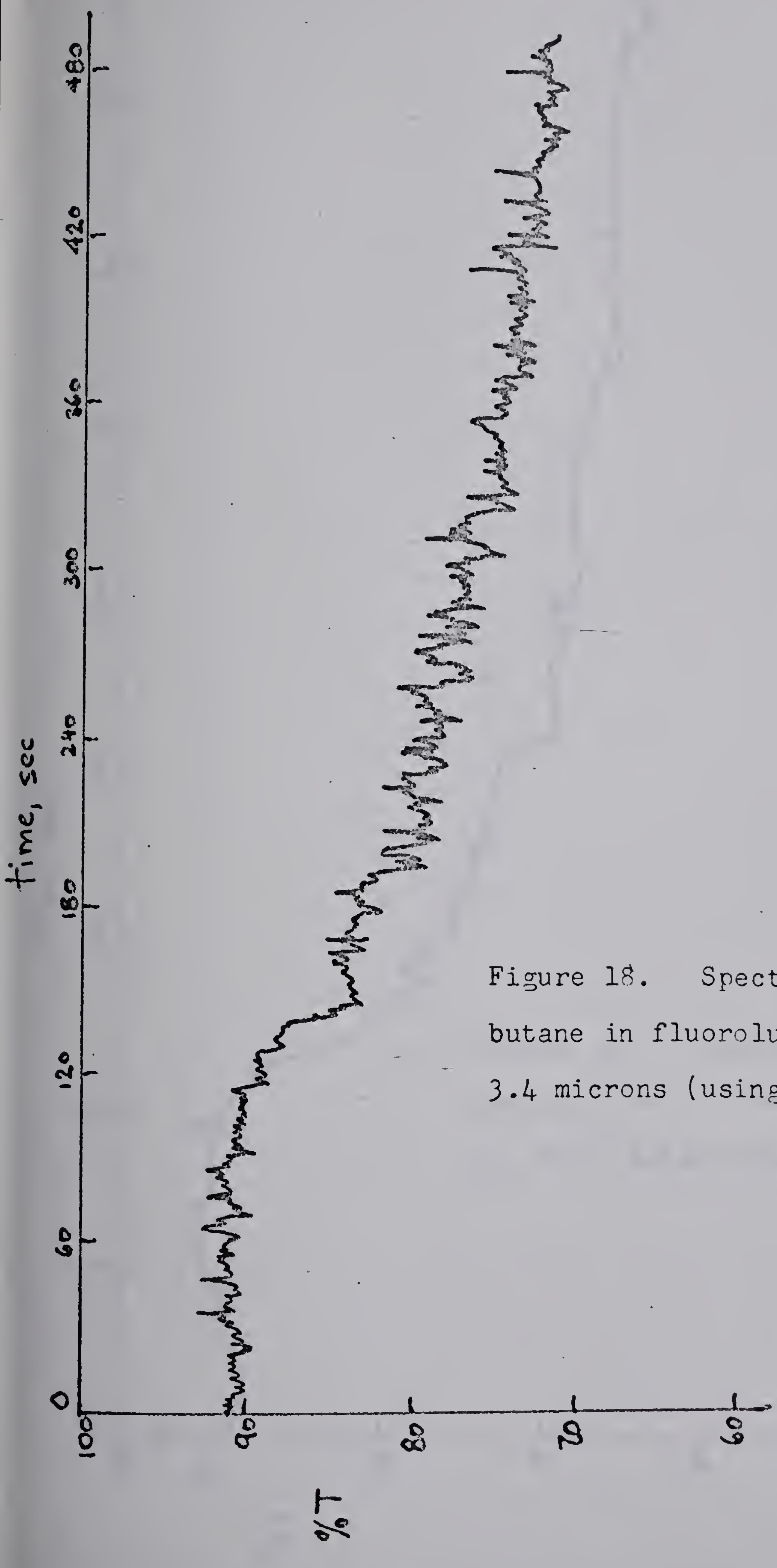

Figure 18. Spectrum of 2-methylbutane in fluorolube at wavelength 3.4 microns (using CC-B, 584 μ spacer).

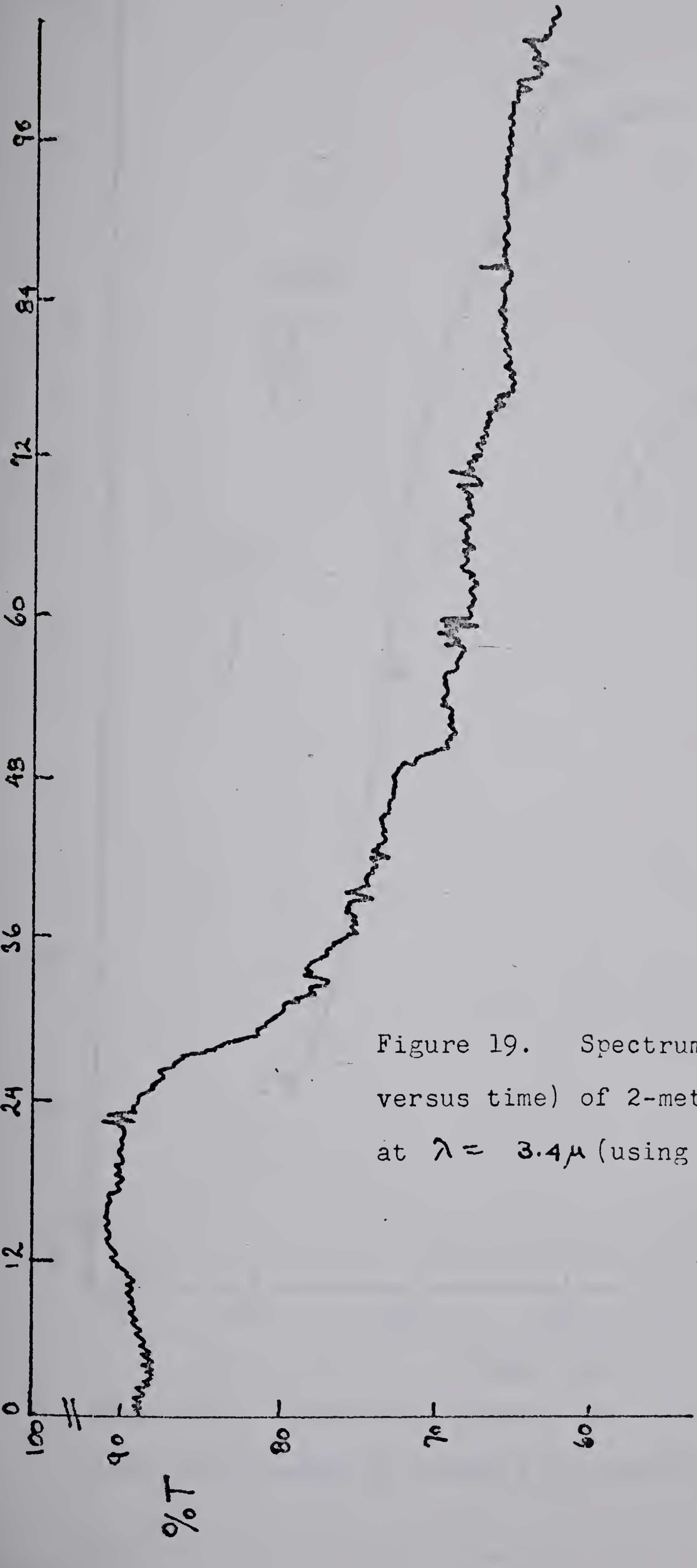

Figure 19. Spectrum (percent transmittance) versus time) of 2-methylbutane in fluorolube at $\lambda = 3.4\mu$ (using CC-B, 381μ spacer).

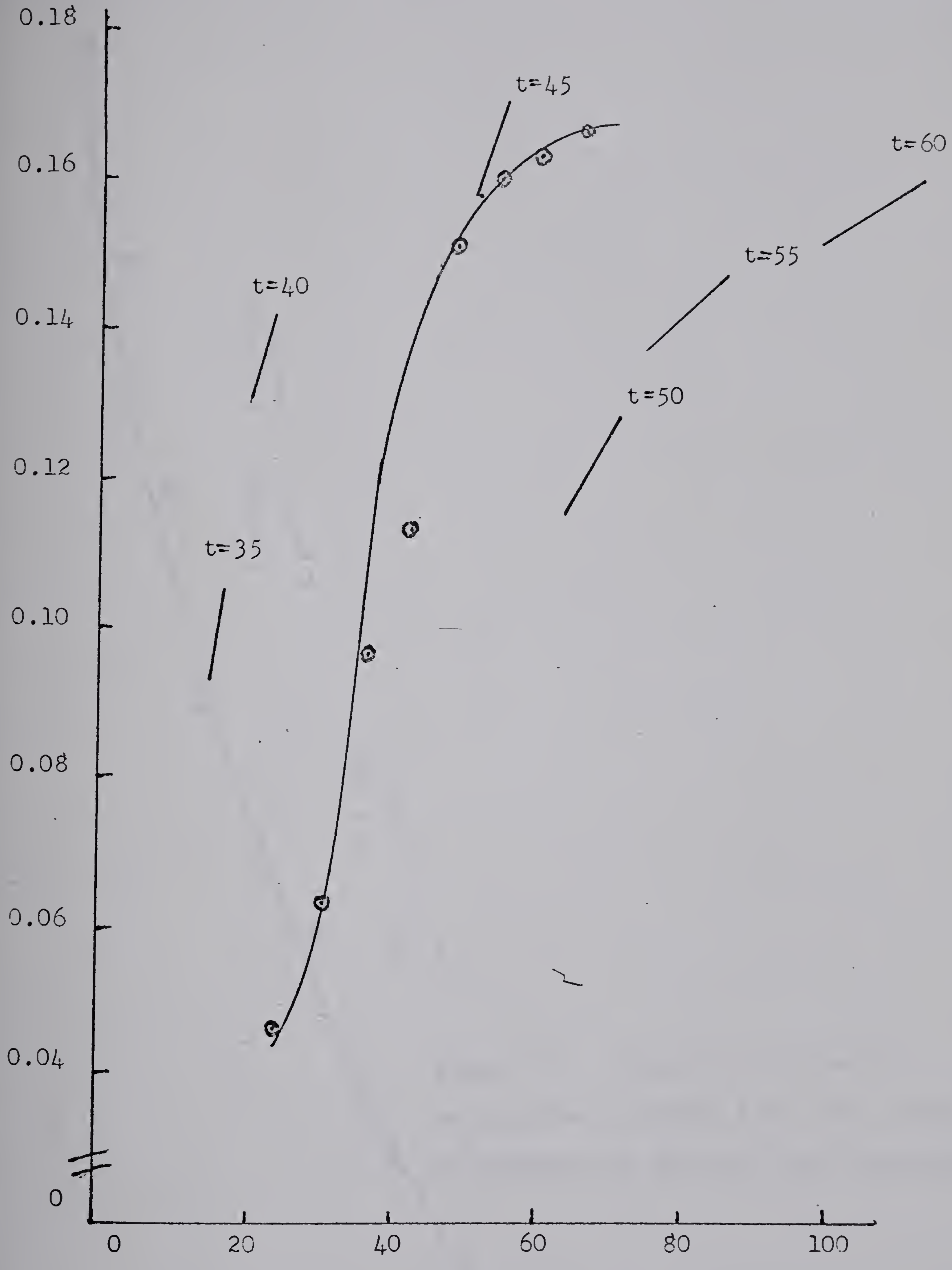

Figure 20. Replot of figure 17 absorbance versus time with slopes of tangents at various times constructed.

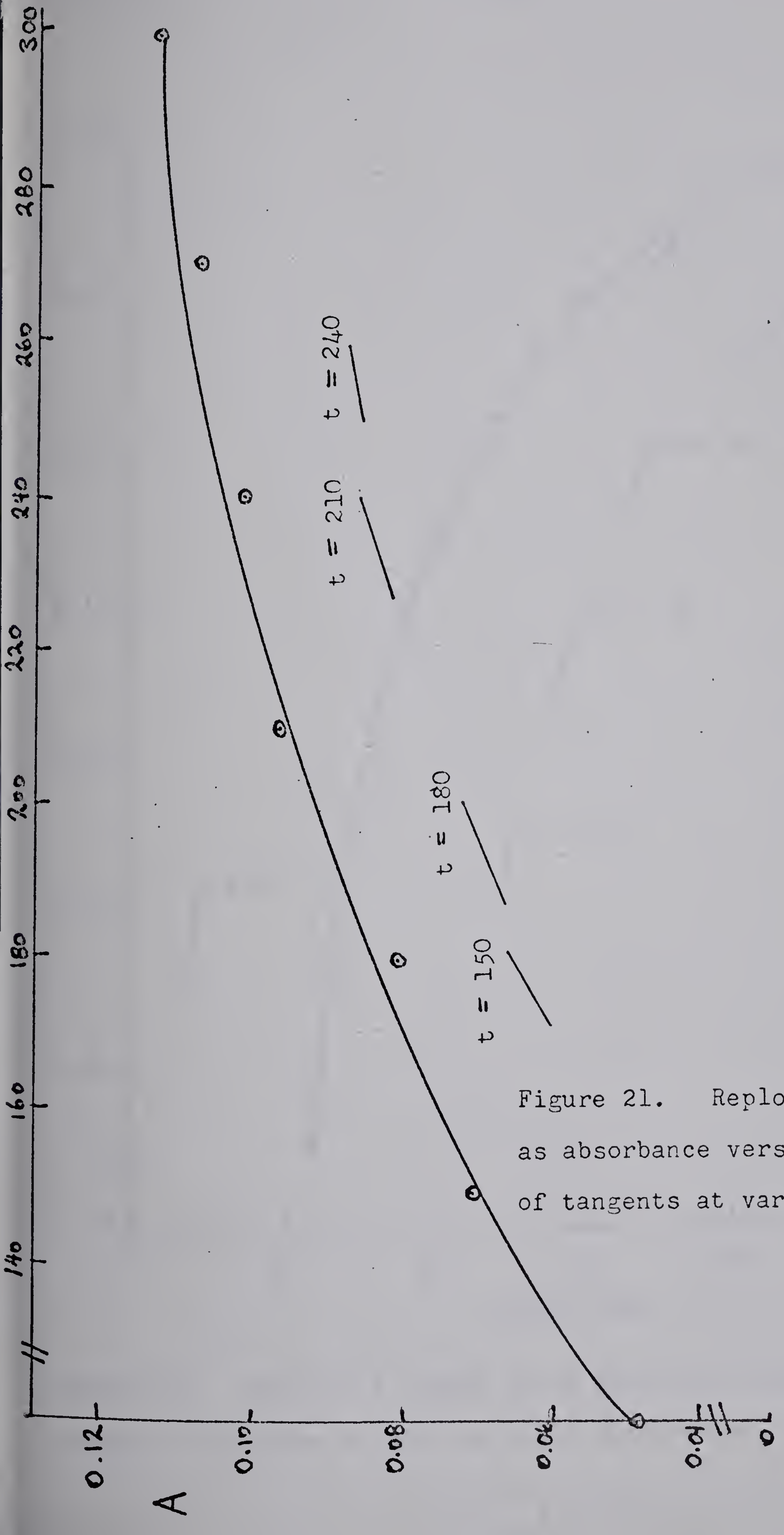

Figure 21. Replot of figure 18 as absorbance versus time with slopes of tangents at various times constructed.

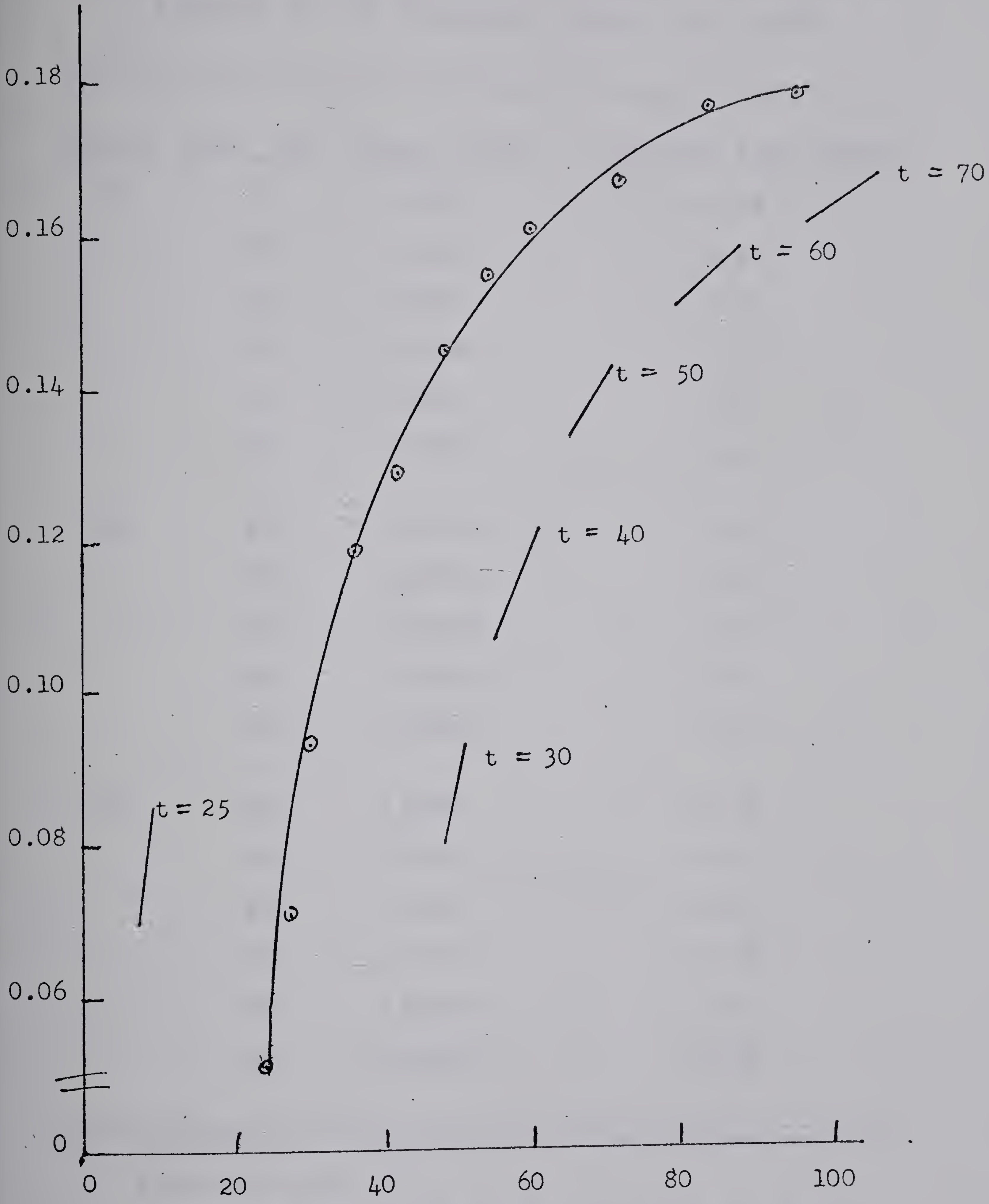

Figure 22. Replot of figure 19 as absorbance versus time with slopes of tangents at various times constructed.

TABLE X. SLOPES (dA/dt) AND LOGARITHMS OF SLOPES OF THE TANGENTS TO THE ABSORBANCE VERSUS TIME PLOTS[a]

Figure	Time, sec	Slope (dA/dt)	Log Slope (log dA/dt)[b]
20	35	0.0066	-2.18
	40	0.0040	-2.40
	45	0.0032	-2.50
	50	0.0018	-2.74
	55	0.0010	-3.00
	60	0.00066	-3.18
21	150	0.00063	-3.20
	180	0.00045	-3.35
	210	0.00035	-3.46
	240	0.000195	-3.71
	270	0.00016	-3.79
22	25	0.0066	-2.18
	30	0.0050	-2.30
	40	0.0026	-2.59
	50	0.00165	-2.78
	60	0.00090	-3.01
	70	0.00063	-3.20

[a] Figures 20, 21, 22.

[b] Log (dA/dt) has been shown previously to be proportional to log (dc/dt) and the two expressions are used interchangeably.

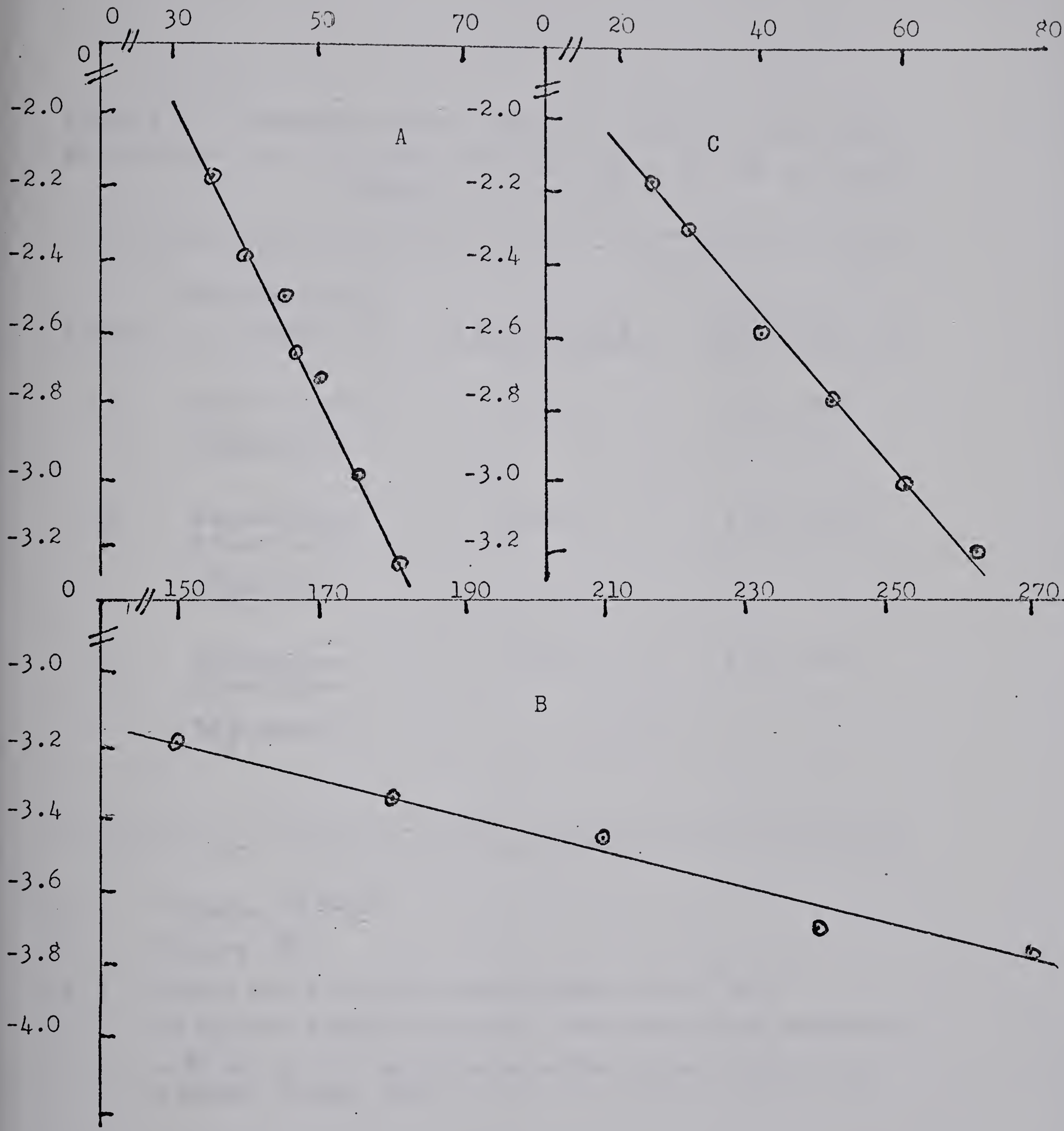

Figure 23. Plots of logdc/dt versus time for the absorbance versus time plots shown in figures 20, 21, 22. The data is taken from Table X.

TABLE X1. DIFFUSION COEFFICIENTS FOR SYSTEMS ILLUSTRATED BY SPECTRA[a] AND CALCULATED FROM THE SLOPES OF THE LOG dA/dt VERSUS TIME PLOTS[b]

Figure	Corresponding System	$-\Delta \log dc/dt / \Delta t$	Diffusion Coefficient [c,d]
-A	ether-fluoro. 254μ spacer	0.040	2.4×10^{-5}
-B	isopentane-fluorolube 584μ spacer	0.005	1.6×10^{-5}
-C	isopentane-fluorolube 381μ spacer	0.024	3.3×10^{-5}

---

a. Figures 17, 18, 19

b. Figure 23

c. Units for diffusion coefficient are $cm^2 sec^{-1}$

d. Diffusion coefficients are calculated from expression $-\pi^2 Dt/ 2.3 h^2$ which equals the slope of plot log (dc/dt) versus time.

TABLE X11. VALUES OF ΔLog (dc/dt)/ Δt AND DIFFUSION COEFFICIENTS FOR 1-PENTENE IN FLUOROLUBE FOUND EXPERIMENTALLY USING CC-B AND SPACER THICKNESSES 127 AND 254 MICRONS

Spacer Thickness	$-\Delta \log(dc/dt)/\Delta t$	Diffusion Coefficient x 10^5 [a]
127μ	0.020	0.30
	0.009	0.13
	0.011	0.17
	0.024	0.36
	0.027	0.41
	0.030	0.45
	0.024	0.36
	0.030	0.45
254μ	0.042	2.5
	0.062	3.7
	0.045	2.7
	0.046	2.8
	0.020	1.2
	0.018	1.1
	0.022	1.3
	0.030	1.8
	0.044	2.7
	0.048	1.7

a. Units cm^2/sec

TABLE X111. VALUES OF $\Delta \text{Log}(dc/dt)/\Delta t$ AND DIFFUSION COEFFICIENTS FOR 1-PENTENE IN FLUOROLUBE FOUND EXPERIMENTALLY USING CC-B AND SPACER THICKNESSES 381 AND 584 MICRONS

Spacer Thickness	$-\Delta \log(dc/dt)/\Delta t$	Diffusion Coefficient x 10^5 [a]
381 μ	0.024	3.3
	0.012	1.6
	0.027	3.6
	0.027	3.6
	0.024	3.3
	0.008	1.1
	0.016	2.2
	0.033	4.3
584 μ	0.005	1.6
	0.011	3.5
	0.009	2.9
	0.012	3.8
	0.012	3.8
	0.014	4.5
	0.012	3.8
	0.007	2.2
	0.005	1.6
	0.012	3.8

a. Units cm^2/sec

TABLE XlV. VALUES OF ΔLog(dc/dt)/Δt AND DIFFUSION COEFFICIENTS FOR 2 METHYLBUTANE IN FLUOROLUBE FOUND EXPERIMENTALLY USING CC-B AND SPACER THICKNESSES 127 AND 254 MICRONS

Spacer Thickness	$-\Delta \log(dc/dt)/\Delta t$	Diffusion Coefficient x 10^5 [a]
127μ	0.047	0.54
	0.029	0.44
	0.022	0.34
	0.054	0.81
	0.032	0.48
	0.023	0.35
	0.030	0.45
	0.014	0.22
	0.020	0.30
	0.034	0.51
254μ	0.042	2.5
	0.028	1.7
	0.030	1.8
	0.034	2.1
	0.028	1.7
	0.040	2.4
	0.028	1.7
	0.038	2.3
	0.027	1.6

a. Units cm^2/sec

TABLE XV. VALUES OF $\Delta \text{Log}(dc/dt)/\Delta t$ AND DIFFUSION COEFFICIENTS FOR 2-METHYLBUTANE IN FLUOROLUBE FOUND EXPERIMENTALLY USING CC-B AND SPACER THICKNESSES 381 AND 584 MICRONS

Spacer Thickness	$-\Delta \log(dc/dt)/\Delta t$	Diffusion Coefficient x 10^5 [a]
381μ	0.024	3.3
	0.014	1.9
	0.024	3.3
	0.026	3.5
	0.023	3.1
	0.020	2.7
	0.019	2.6
	0.016	2.2
584 μ	0.006	1.9
	0.007	2.2
	0.004	1.3
	0.005	1.6
	0.004	1.3
	0.003	1.0

a. Units cm^2/sec

TABLE XV1. VALUES OF ΔLog(dc/dt)/ Δt AND DIFFUSION COEFFICIENTS FOR DIETHYL ETHER IN FLUOROLUBE FOUND EXPERIMENTALLY USING CC-B AND SPACER THICKNESSES 127 AND 254 MICRONS

Spacer Thickness	$-\Delta\log(dc/dt)/\Delta t$	Diffusion Coefficient x 10^5 [a]
127 μ	0.036	0.54
	0.022	0.33
	0.026	0.39
	0.028	0.42
	0.034	0.51
	0.024	0.36
	0.034	0.51
	0.017	0.26
	0.017	0.26
	0.030	0.45
254 μ	0.022	1.3
	0.039	2.4
	0.032	1.9
	0.040	2.4
	0.034	2.1
	0.027	1.6
	0.036	2.2
	0.040	2.4
	0.032	1.9

a. Units cm^2/sec

TABLE XV11. VALUES OF Δ Log (dc/dt)/Δ t AND DIFFUSION COEFFICIENTS FOR DIETHYL ETHER IN FLUOROLUBE FOUND EXPERIMENTALLY USING CC-B AND SPACER THICKNESSES 381 AND 584 MICRONS

Spacer Thickness	$-\Delta$log (dc/dt)/Δ t	Diffusion Coefficient x 10^5 [a]
381	0.013	1.8
	0.017	2.3
	0.019	2.6
	0.023	3.1
	0.014	1.9
	0.018	2.4
	0.017	2.3
584	0.011	3.5
	0.011	3.5
	0.006	1.9
	0.007	2.2
	0.009	2.9
	0.010	3.2

a. Units cm^2/sec

TABLE XV111. SUMMARY OF VALUES OF DIFFUSION COEFFICIENTS FOR 1-PENTENE, 2-METHYLBUTANE AND DIETHYL ETHER IN FLUOROLUBE

Solute	Average Diffusion Coefficient x 10^{5a}	Average Deviation x 10^5	Standard Deviation x 10^5
1-pentene	2.7	0.9	1.0
2-Me-butane	2.2	0.6	0.7
di-Et-ether	2.4	0.4	0.6

a. Units cm^2/sec

TABLE X1X. VALUES OF DIFFUSION COEFFICIENTS FOR ACETONE CARBOWAX 600, CARBOWAX 1500, SILICONE GREASE, DINONYL-PHTHALATE AND UCON

Solvent	Spacer Thickness	Diffusion Coefficient x 10^{5} cm^{2}/sec
Carbowax 600	127μ	0.12
		0.060
		0.070
	381μ	1.5
		2.1
		1.2
Carbowax 1500	127μ	0.030
		0.040
Silicone Grease	127μ	0.12
		0.060
		0.98
Dinonyl-phthalate	127μ	0.068
		0.15
		0.18
	381μ	1.7
		1.7
Ucon (-50-HB 280X)	127μ	0.065
		0.060
		0.15
	381μ	1.9
		1.7

are presented in Table X. The plots of log slope versus time are shown in figure 23 and the results, i.e., slopes of lines and calculated diffusion coefficients, are shown in Table X1.

The slopes of the log dc/dt versus t plots and the calculated diffusion coefficients for the 1-pentene--fluorolube, 2-methylbutane--fluorolube and diethyl ether--fluorolube systems are presented in Tables X11 - XV111 inclusive. Final tabulation of results as averages, average deviations and standard deviations for the fluorolube systems is given in Table XV111.

From the spectra it was seen that as the spacer thickness increased, the change in absorption or the equilibrium concentration decreased.

Similar data and results for the acetone--Carbowax 600, Carbowax 1500, silicone grease, DNP and Ucon systems are presented in Table X1X.

111-2 Discussion

The theoretical model of diffusion into a slab coupled with Fick's second law of diffusion lead to a simple expression for the diffusion coefficient as a function of the change of concentration with time at a given distance in the slab. This change of concentration is easily measured by internal reflectance spectroscopy. So it appears that the method outlined in this work should yield fairly accurate values for the diffusion coefficients. However,

the absence of diffusion data in the literature, especially for the systems such as those present in gas chromatography, makes it difficult to affirm the values of D derived experimentally.

The data which appears in Tables X11-XV11 inclusive shows the discrepancy in values measured for all samples using the 127 micron spacer with respect to those values measured at higher spacer widths. The data, which showed lower values for the diffusion coefficients, was deleted for the final analysis and was not entered into Table XV111. There are two possible sources of error for thin layers, i.e., non-uniformity of the film and surface effects. The uniformity of the film cannot be guaranteed, particularly not for very thin layers of liquids. Liquids such as fluorolube, DNP and Ucon can flow, and whether this flow is caused by movement of the cell, or by the flow of gas in the cavity, this flow of liquid is more important for thin layers. If the solute lowers the surface tension of the solvent, the solute will tend to be more concentrated at the surface of the layer. This effect would give values of the diffusion coefficient lower than expected. Since thicker layers appeared to be more stable in preparation and since the surface effect was expected to have smaller influence on the results for thicker layers, only data obtained from

measurements with 254μ, 381μ, and 584μ from Tables X11-XV11 were considered in the calculation of diffusion coefficients.

The author could not explain the appearance of the spectra with regard to decreasing equilibrium concentration with increasing spacer thickness as mentioned in section 111-1. A study was made using a solution of known concentration to see if spacer thickness had any effect on the absorption. With all spacers tried the absorption was the same. This is also expected in the measurement of diffusion coefficients, i.e., the equilibrium concentration should be independent of spacer thickness. Thus no explanation for this anomalous behaviour is offered.

The results for each solute-fluorolube system were averaged and the average deviation and standard deviation calculated. These results were recorded in Table XV111. Because the standard deviation is large, the diffusion coefficients measured cannot be considered quantitative. However some qualitative observations can be made.

The Wilke-Chang equation, considered by Giddings (10) to be one of the best empirical expressions for diffusion coefficients, $D = 7.4 \times 10^{-8} (xM)^{\frac{1}{2}} T/\eta V^{0.6}$ was used to try to estimate the predicted values for the 1-pentene--fluorolube system. The viscosity of fluorolube at 100°F

($\sim 38^oC$) (27) was 100 centistokes - as centistokes times density equals centipoise, and the density is given for 100^oF as 1.92 gm/ml, the viscosity in centipoise is found to be 192. The average molecular weight of fluorolube was taken to be 775. Taking the molal volume of 1-pentene as 111 (from values in Table lV), the Wilke-Chang equation gives the diffusion coefficient at 100^oF as about 2×10^{-7} cm^2/sec. The value at 25^oC will be less than 2×10^{-7} because of the increase in viscosity with decrease in temperature. The Wilke-Chang estimate is lower than the experimental values found. A similar case was reported in the literature when the values for the diffusion coefficient for the isobutylene--DNP system investigated by Houghton et. al. (15) , D for temperature range 0 - 75^oC were 0.026 - 0.61 x $10^5 cm^2/sec$, were higher than the Wilke-Chang estimates by factors of 11 to 44. Giddings writes (12) "Thus until further evidence is available, calculations regarding small solute molecules in large molecules of gas liquid chromatography are suspect."

Although the Wilke-Chang equation does not give a good estimate of the experimentally measured diffusion coefficients, qualitative relationships can be made using the Wilke-Chang proportionality $D \propto 1/V^{0.6}$. The molal volumes for 2-methylbutane and diethyl ether were calculated from Table lV (118 and 107 respectively), and the

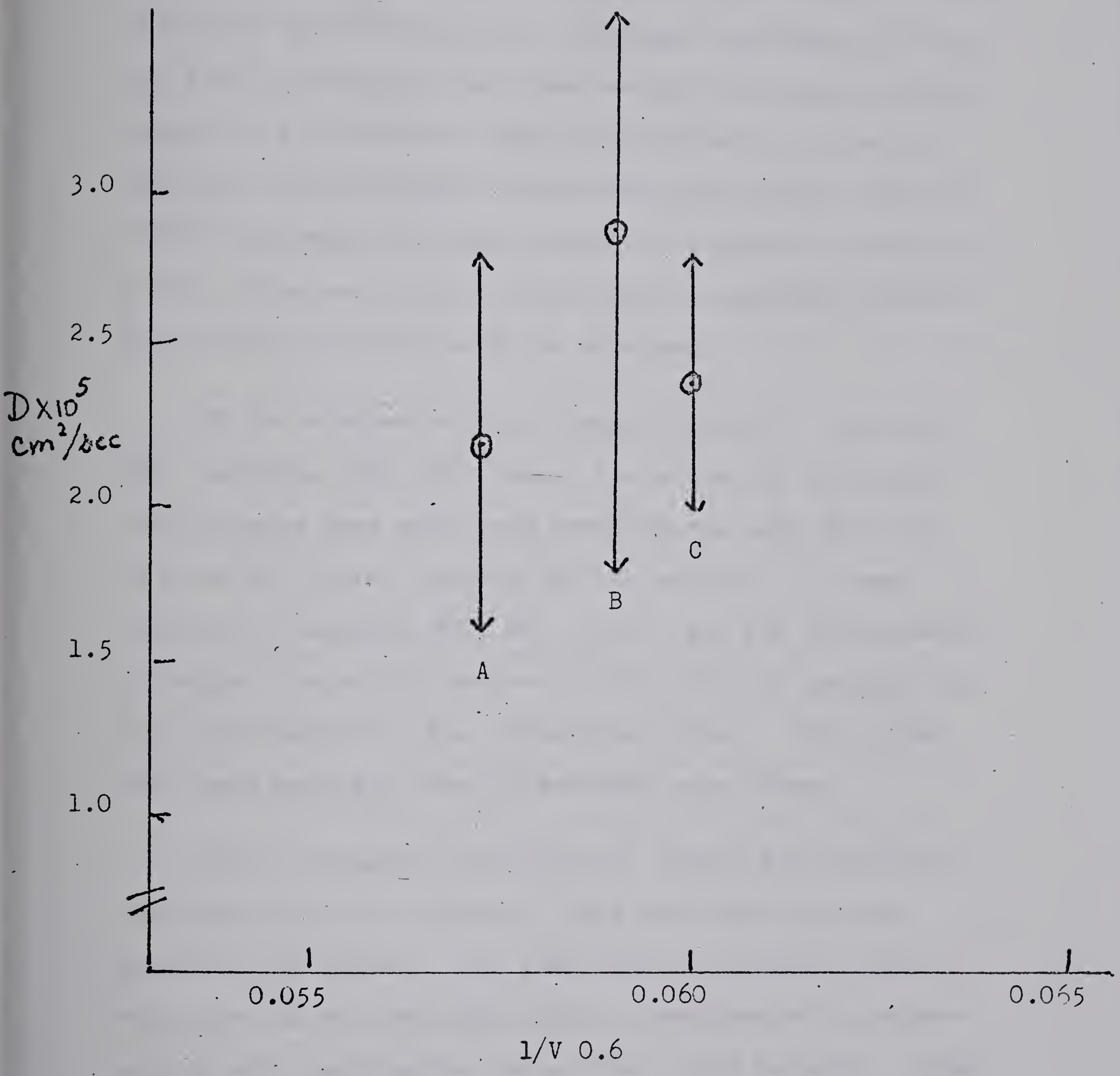

Figure 24 Wilke-Chang Depencence of D on 1/V 0.6: A 2-methylbutane; B 1-pentene; C diethylether.

values of experimental diffusion coefficients and range defined by the average deviations were plotted against the values of $1/V^{0.6}$ (fig. 24). Although the three points do not form a straight line, considering the range of values caused by the deviation there appears to be a trend to show that the diffusion coefficient is a linear function $1/V^{0.6}$ and that if a large number of solutes of varying molal volume were run in fluorolube, a variation of the Wilke-Chang equation might be obtained.

Of the acetone-solvent series (solvents - Carbowax 600, Carbowax 1500, DNP, etc.) the values of diffusion coefficients were made from measurements with both the 127 and 381 micron spacers for the solvents of lower viscosity (Carbowax 600, DNP, Ucon); and for the solvents of higher viscosity (Carbowax 1500, Silicone grease) runs were only made with the 127 micron spacer. Only a few runs were made and thus no averages were taken.

Since viscosity and molecular weight data were not available for all solvents - only available for the acetone--DNP system - and since the Wilke-Chang equation was shown to be unreliable from a quantitative consideration, only qualitative comparisons could be made. Using the data for acetone--DNP, acetone--Carbowax 600, and acetone--Carbowax 1500, comparison was made on the basis

of the Wilke-Chang dependence of D on $M^{\frac{1}{2}}/\eta$ and estimates of the viscosities of the carbowaxes were made. The diffusion coefficient for the acetone--DNP system was found to be 1.7×10^{-5} cm^2/sec and was about the same as the value for diffusion of acetone in Carbowax 600 (average 1.6×10^{-5} cm^2/sec). The value for this latter system is about fifty times as large as the diffusion coefficient for the Carbowax 1500 system. From the viscosity of dinonylphthalate, 81 centipoise at 25°C (15), and the molecular weight the ratio $M^{\frac{1}{2}}/\eta$ was found to be about 0.25. Thus this ratio for the Carbowax 600 system should be the same and for the Carbowax 1500 system it should be 0.005 - if the Wilke-Chang dependancy is applicable. From this ratio the viscosities of the carbowaxes were estimated: for Carbowax 600 viscosity $\sim$100, for Carbowax 1500 viscosity $\sim$ 4700 (values in centipoise). Although the viscosities for the carbowaxes are not known at 25°C, the values found by using the Wilke-Chang dependence of diffusion coefficient on molecular weight and viscosity give values which appear to be in agreement with the properties observed while handling these reagents. Carbowax 600 is liquid with pouring qualities much like those of DNP as is expected with viscosity of 100 centipoise; Carbowax 1500 is a waxy solid which is also expected from its high value of viscosity.

In the measurement of diffusion coefficients and qualitative comparisons with the Wilke-Chang equation no mention was made of temperature effects. The dependence of diffusion coefficients on temperature in the Wilke-Chang relation is shown to be two fold, i.e., D is directly proportional to T, and the D is inversely proportional to viscosity which is in turn inversely proportional to the temperature. The change of viscosity with temperature is great especially for high molecular weight solvents. Thus any change in temperature during the course of the experiment would cause a change in the value of D calculated. Since with infrared spectroscopy the sample heats up during the scan (more for thick layers than for thin), the values of the diffusion coefficients would be higher than those expected from the Wilke-Chang equation.

These comparisons offer a qualitative confirmation of the values of diffusion coefficients found in this work.

111-3 Errors

There are sources of error which are inherent in the method;/the replotting of data of percent transmittance as absorption data, the construction of curves and tangents, and the measurements of slopes. The error in replotting data is dependent on the value of % T being converted.

The spectra could be read to the nearest 0.5%T and in Table XX percent error in absorbance is shown at various values of %T. From this table it can been seen that at high and low values of %T the percent error in absorbance rises. The error in the construction of curves and tangents and in measuring slopes was estimated by having the data replotted independently and comparing the slopes of the log (dc/dt) versus time plots with those measured by the author. The results of this replotting and comparison with the author's results are shown in Table XXl along with an estimate of the percent error between the two sets of results.

The main source of error in this procedure arises from the preparation of the solvent layer. There can be no guarantee as to the uniformity and actual thickness of the layers, especially when using the thinner spacers. Overflow, and leakage under the spacer due to non-uniformity of the grease seal can be controlled to some extent, but these can occur causing variation in the layer thickness and consequently variation in the value of the diffusion coefficient.

Another source of error which was mentioned previously is temperature and the heating of the solvent layer during the spectroscopic measurement of diffusion coefficients. One way in which this could be controlled would be the use of a filter which would cut out the radiation less than

TABLE XX. ERRORS IN ABSORBANCE DUE TO TRANSFORMATION OF DATA FROM PERCENT TRANSMITTANCE TO ABSORBANCE UNITS[a]

Reading %T	Absorbance	Absolute error	Percent error
5	1.301	0.040	3.1%
10	1.000	0.023	2.4%
20	0.699	0.009	1.3%
30	0.522	0.006	1.2%
50	0.301	0.004	1.4%
70	0.155	0.003	2.0%
90	0.045	0.004	9.7%

[a] $A = \log 1/T$

two microns (the bulk of the energy emitted by the black body source.

Despite these sources of error, this method does give reasonable values of diffusion coefficients and appears to be a good method for determining them. The accuracy of these numbers could be improved by changing aspects of the procedure and cell design. The use of thicker spacers - of the order of one millimeter - should reduce many problems in non-uniformity of layer and possible reduction of surface effects. These thicker spacers should also make it easier to apply a more uniform and reproducible layer of solvent. The use of teflon as spacer material instead of metal would improve the contact between the prism-plate and the spacer and would eliminate the need for a grease seal. If the spacer were glued onto the plate, the need for a cell cover such as CC-A would be eliminated and the length of time required for an individual run would be decreased.

TABLE XXl. ERRORS FOUND IN REPLOTTING OF DATA

	Slope of log (dc/dt) versus t plot		Percent Error
Measurement	1	11	
A	0.007	0.008	14
B	0.034	0.028	21
C	0.011	0.0085	34
D	0.028	0.024	17
E	0.014	0.017	21
F	0.014	0.017	21
G	0.026	0.023	13
H	0.027	0.023	17
I	0.028	0.032	14

lV CONCLUSION

Using theoretical background of diffusion as given by Fick's law and Jost (16), and the technique of FMIR, a method for the determination of liquid diffusion coefficients was worked out. Two cell covers for the FMIR solid sampling cell, CC-A and CC-B, were designed to provide uniform liquid films of known thicknesses; and the sampling system was designed to provide constant flow of sample in the gas phase to the layer. Using a Perkin-Elmer IR-137 on its side to allow horizontal placement of the prism-plates, diffusion coefficients for systems of different solutes in single solvent and one solute in different solvents were measured by following the change of concentration with time as indicated by the spectra. Although the data cannot be compared to literature values, they are consistent with approximations given by authors such as Perrett (19) and Bohemen and Purnell (3). The values obtained and that could be obtained by this method will help elucidate liquid phase mass transfer terms in gas chromatography.

BIBLIOGRAPHY

(1) J.K. Barr and D.R. Sawyer. Anal. Chem. 36, 1753 (1964)

(2) R.P. Bauman. "Absorption Spectroscopy." John Wiley and Sons, Inc., New York (1963)

(3) J. Bohemen and J.H. Purnell. J. Chem. Soc. 360, 2630 (1961)

(4) "Handbook of Chemistry and Physics." Chem Rubber Pub. Co., Cleveland, U.S.A., 40th Edition

(5-a) "Attenuated Total Reflectance." Connecticut Instrument Corp.

(5-b) "The ATR Spectra of Rubber and Rubber Formulations." Connecticut Instrument Corp.

(6) J. Crank. "The Mathematics of Diffusion." Oxford, London (1956).

(7) J.E. Evanoff. MSc. Thesis, University of Alberta, (1965)

(8) J. Fahrenfort. Spectrochimica Acta 17, 698 (1961)

(9) J.C. Giddings "Dynamics of Chromatography," Part 1, Marcel Dekker, Inc., New York (1965), p. 229.

(10) ibid,, p. 233

(11) ibid., p. 233-234

(12) ibid., p. 237

(13) M.J.E. Golay in "Gas Chromatography, 1958," D.M. Desty, ed., Academic Press, New York (1958), p. 36.

(14) N.J. Harrick. Ann N.Y. Acad. Sci. 101, 928 (1963)

(15) G. Houghton, A.S. Kesten, J. E. Funk, and J. Coull. J. Phys. Chem. 65, 653 (1961)

(16) W. Jost. "Diffusion in Solids, Liquids, Gases," Third Printing, Academic Press, New York (1960) pp. 32-37.

(17) ibid., p. 36

(18) S.D. Nogare and L.W. Safranski. "Gas Chromatography" in "Organic Analysis," Vol. lV, Interscience Publishers Inc., New York (1960)

(19) R.H. Perrett. Anal. Chem. 37, 1342 (1965).

(20) J.M. Purnell "Gas Chromatography." John Wiley and Sons, Inc., New York (1962). pp. 124-125

(21) ibid., p. 127

(22) J.J. Van Deemter, F.J. Zuiderweg, and A. Klinkenberg, Chem. Eng. Sci. 5, 271 (1956)

(23) C.R. Wilke and Pin Chang. A.I. Ch. E. Journal 7, 264 (1955)

(24) "Commentary" no. 9, Wilks Scientific Corp, Feb. (1966)

(25) "Internal Reflectance Spectroscopy", Vol. 1, Wilks Scientific Corp, (1965)

(26) "Techniques in MIR," No. 1, Wilks Scientific Corp, (1966)

(27) Hooker Electrochemical Co. Manual (1965)

B29876